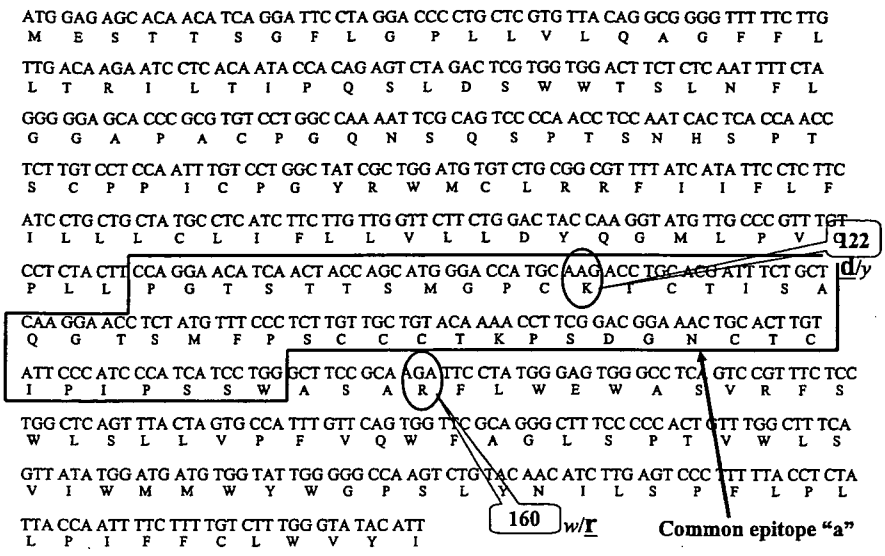

Figure 2 Predicted amino acid sequence of the surface region of the HBV genome obtained from sera before and 25 weeks after the initiation of interferon and ribavirin treatment, at which time the anti-HBs titer was at a maximum (DDBJ accession number: AB284371). The sequence was 100% identical, which was also the case for another region of HBV-DNA (data not shown). Epitope determinant regions; box, a determinant; 122, d/y; 160, w/r, are shown. Nucleotide sequences indicated that the HBsAg subtype was adr.

type HBV-DNA.[14,15] Two HBV isolates obtained before and after interferon/ribavirin treatment in the present study have in common three unique mutations leading to amino acid changes (Thr to Met at position 118, Pro to Ser at 127, Phe to Ser at 158) (Fig. 2). These amino acid changes were not listed in the previous report, which showed that changes at 144 and 145 were the possible epitope determinant of d/y other than the main d/y determinant at 122.[14] In addition, these three mutations are not included in those which are associated with the failure of diagnostic tests of HBsAg or with vaccine or immunoglobulin therapy escape.[15] Consequently, there seemed to be no amino acid changes in the HBV-DNA that might weaken HBsAg epitope in each subtype determinant.

Inhibition testing of anti-HBs using several purified antigens showed that only the adr antigen significantly inhibited anti-HBs, whereas neither the adw nor the ay antigen did so, and thus the main reactivity of the anti-HBs seems to be against the r epitope (Fig. 3). In addition, the serum with a high titer of anti-HBs did not react significantly with other anti-HBs measuring kits using the ad and ay epitopes (Abbott, Tokyo, Japan; data not shown), confirming the result of the inhibition test. Because we did not perform a precise epitope-mapping analysis against the anti-HBs using multiple synthesized oligopeptides that could cover the whole HBsAg region, this result remains inconclusive and the anti-HBs activities could still be against as-yet-undefined epitopes. However, it may not be an over-interpretation to suggest that the appearance of anti-HBs was a break in immune tolerance against some epitopes in HBsAg induced by the interferon/ribavirin treatment, because we could not detect any amino acid changes by the treatment.

The characteristic upsurge in anti-HBs titer during interferon treatment was specific to this patient, who also received ribavirin. Seven other chronic hepatitis B patients who received interferon monotherapy were found not to have significant changes in anti-HBs titer in response to the initiation of interferon therapy (Table 1). Thus, the appearance of anti-HBs seemed to be due to the effect of ribavirin, which has an immunomodulative function as well as a mutagenic

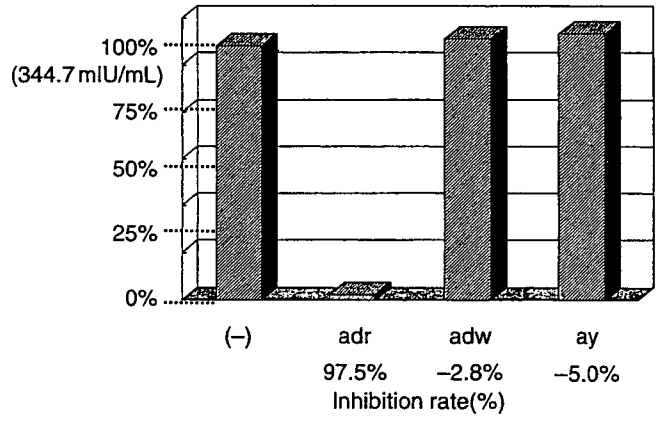

Figure 3 Inhibition test for anti-HBs reactivity using several subtype-specific antigens. Purified adr, adw and ay antigens were added to the serum with a high anti-HBs titer. The anti-HBs titer of the serum used for this experiment is shown as 100% and the maximum inhibition percentage values obtained by each antigen are shown. Minus (–) means adding no antigen.

effect on the virus.[11] In addition, the decrease in anti-HBs and a reciprocal increase in HBsAg titer occurred after the cessation of ribavirin (Fig. 1), despite the continuation of interferon that constituted the major antiviral component of the combination therapy, supporting the idea that the break in immune tolerance against HBsAg resulted from the immune-modulating activities of ribavirin. This observation was made in a single patient and was incidental to a situation where ribavirin was used to treat a coinfection with hepatitis C. Should we come across a similar clinical situation of coinfection with HBV and HCV, and treatment with interferon and ribavirin is given, the patient should be carefully monitored to determine whether or not such a serological phenomenon occurs again and results in a good clinical outcome for chronic HBV infection. A clinical study should be commenced if these findings can be confirmed.

ACKNOWLEDGMENTS

WE THANK DR Niitsuma (Fujirebio) for technical help with the anti-HBs test of anti-HBs and Ms Naomi Cho for her technical assistance.

REFERENCES

1 Liaw YF, Sheen IS, Chen TJ, Chu CM, Pao CC. Incidence, determinants and significance of delayed clearance of serum HBsAg in chronic hepatitis B virus infection: a prospective study. *Hepatology* 1991; 13: 627–31.
2 Kohno H, Inoue T, Tsuda F, Okamoto H, Akahane Y. Mutations in the envelope gene of hepatitis B virus variants co-occurring with antibody to surface antigen in sera from patients with chronic hepatitis B. *J Gen Virol* 1996; 77: 1825–31.
3 Yamamoto K, Horikita M, Tsuda F *et al.* Naturally occurring escape mutants of hepatitis B virus with various mutations in the S gene in carriers seropositive for antibody to hepatitis B surface antigen. *J Virol* 1994; 68: 2671–6.
4 Ackerman Z, Wands JR, Gazitt Y, Brechot C, Kew MC, Shouval D. Enhancement of HBsAg detection in serum of patients with chronic liver disease following removal of circulating immune complexes. *J Hepatol* 1994; 20: 398–404.
5 Ogata N, Ostberg L, Ehrlich PH, Wong DC, Miller RH, Purcell RH. Markedly prolonged incubation period of hepatitis B in a chimpanzee passively immunized with a human monoclonal antibody to the a determinant of hepatitis B surface antigen. *Proc Natl Acad Sci USA* 1993; 90: 3014–18.
6 Okamoto H, Imai M, Tsuda F, Tanaka T, Miyakawa Y, Mayumi M. Point mutation in the S gene of hepatitis B virus for a d/y or w/r subtypic change in two blood donors carrying a surface antigen of compound subtype adyr or adwr. *J Virol* 1987; 61: 3030–4.
7 Okamoto H, Imai M, Miyakawa Y, Mayumi M. Site-directed mutagenesis of hepatitis B surface antigen sequence at codon 160 from arginine to lysine for conversion of subtypic determinant from r to w. *Biochem Biophys Res Commun* 1987; 148 (1): 500–4.
8 Okamoto H, Yano Y, Nozaki A *et al.* Mutations within the S gene of hepatitis B virus transmitted from mothers to babies immunized with hepatitis B immune globulin and vaccine. *Pediatr Res* 1992; 32: 264–8.
9 Pawlotsky JM. Current and future concepts in hepatitis C therapy. *Semin Liver Dis* 2005; 25: 72–83.
10 Crotty S, Cameron CE, Andino R. RNA virus error catastrophe: direct molecular test by using ribavirin. *Proc Natl Acad Sci USA* 2001; 98: 6895–900.
11 Ning Q, Brown D, Parodo J *et al.* Ribavirin inhibits viral-induced macrophage production of TNF, IL-1, the procoagulant fgl2 prothrombinase and preserves Th1 cytokine production but inhibits Th2 cytokine response. *J Immunol* 1998; 160: 3487–93.
12 Kato N, Hasegawa K, Torii N, Yamauchi K, Hayashi N. A molecular analysis of viral persistence in surface antigen –negative chronic hepatitis B. *Hepatology* 1996; 23: 389–95.
13 Tang JH, Yeh CT, Chen TC, Hsieh SY, Chu CM, Liaw YF. Emergence of an S gene mutant during thymosin alpha 1 therapy in a patient with chronic hepatitis B. *J Infect Dis* 1998; 178: 866–9.
14 Okamoto H, Omi S, Wang Y *et al.* The loss of subtypic determinant in alleles, d/y or w/r, on hepatitis B surface antigen. *Mol Immunol* 1989; 26: 197–205.
15 Avellon A, Echevarria JM. Frequency of Hepatitis B virus "a" determinant variants in unselected Spanish chronic carriers. *J Med Virol* 2006; 78: 24–36.

doi:10.1111/j.1440-1746.2007.05076.x

HEPATOLOGY

Inhibition of hepatitis C virus infection and expression *in vitro* and *in vivo* by recombinant adenovirus expressing short hairpin RNA

Naoya Sakamoto,*,† Yoko Tanabe,* Takanori Yokota,‡ Kenichi Satoh,§ Yuko Sekine-Osajima,* Mina Nakagawa,*,† Yasuhiro Itsui,* Megumi Tasaka,* Yuki Sakurai,* Chen Cheng-Hsin,* Masahiko Yano,¶ Shogo Ohkoshi,¶ Yutaka Aoyagi,¶ Shinya Maekawa,†† Nobuyuki Enomoto,†† Michinori Kohara§ and Mamoru Watanabe*

Departments of *Gastroenterology and Hepatology, †Hepatitis Control, and ‡Neurology and Neurological Science, Tokyo Medical and Dental University, §Department of Microbiology and Cell Biology, The Tokyo Metropolitan Institute of Medical Science, Tokyo, ¶Gastroenterology and Hepatology Division, Graduate School of Medical and Dental Sciences, Niigata University, Niigata, and ††First Department of Medicine, Yamanashi University, Yamanashi, Japan

Key words
adenovirus vector, hepatitis C virus, RNA interference.

Accepted for publication 12 April 2007.

Correspondence
Dr Naoya Sakamoto, Department of Gastroenterology and Hepatology, Tokyo Medical and Dental University, 1-5-45 Yushima, Bunkyo-ku, Tokyo 113-8519, Japan.
Email: nsakamoto.gast@tmd.ac.jp

NS and YT have contributed equally to this paper.

Abstract

Background and Aim: We have reported previously that synthetic small interfering RNA (siRNA) and DNA-based siRNA expression vectors efficiently and specifically suppress hepatitis C virus (HCV) replication *in vitro*. In this study, we investigated the effects of the siRNA targeting HCV-RNA *in vivo*.

Methods: We constructed recombinant retrovirus and adenovirus expressing short hairpin RNA (shRNA), and transfected into replicon-expressing cells *in vitro* and transgenic mice *in vivo*.

Results: Retroviral transduction of Huh7 cells to express shRNA and subsequent transfection of an HCV replicon into the cells showed that the cells had acquired resistance to HCV replication. Infection of cells expressing the HCV replicon with an adenovirus expressing shRNA resulted in efficient vector delivery and expression of shRNA, leading to suppression of the replicon in the cells by ~10^{-3}. Intravenous delivery of the adenovirus expressing shRNA into transgenic mice that can be induced to express HCV structural proteins by the Cre/*lox*P switching system resulted in specific suppression of virus protein synthesis in the liver.

Conclusion: Taken together, our results support the feasibility of utilizing gene targeting therapy based on siRNA and/or shRNA expression to counteract HCV replication, which might prove valuable in the treatment of hepatitis C.

Introduction

Hepatitis C virus (HCV), which affects 170 million people worldwide, is one of the most important pathogens causing liver-related morbidity and mortality.[1] The difficulty in eradicating HCV is attributable to limited treatment options against the virus and their unsatisfactory efficacies. Even with the most effective regimen with pegylated interferon (IFN) and ribavirin in combination, the efficacies are limited to less than half of the patients treated.[2] Given this situation, the development of safe and effective anti-HCV therapies is one of our high-priority goals.

RNA interference (RNAi) is a process of sequence-specific, post-transcriptional gene silencing that is initiated by double-stranded RNA.[3,4] Because of its potency and specificity, RNAi rapidly has become a powerful tool for basic research to analyze gene functions and for potential therapeutic applications. Recently, successful suppression of various human pathogens by RNAi have been reported, including human immunodeficiency viruses,[5,6] poliovirus,[7] influenza virus,[8] severe acute respiratory syndrome (SARS) virus[9] and hepatitis B virus (HBV).[10–13]

We and other researchers have reported that appropriately designed small interfering RNA (siRNA) targeting HCV genomic RNA can efficiently and specifically suppress HCV replication *in vitro*.[14–19] We have tested siRNA designed to target the well-conserved 5′-untranslated region (5′-UTR) of HCV-RNA, and identified the most effective target, just upstream of the translation initiation codon. Furthermore, transfection of DNA-based vectors expressing siRNA was as effective as that of synthetic siRNA in suppressing HCV replication.[14]

In this study, we explored the further possibility that efficient delivery and expression of siRNA may be effective in suppression and elimination of HCV replication and that delivery of such

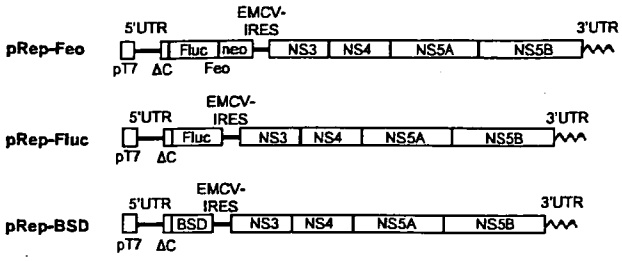

Figure 1 Structures of HCV replicon plasmids. The pRep-Feo expressed a chimeric reporter protein of firefly luciferase (Fluc) and neomycin phosphotransferase (GenBank accession No. AB119282).[14,20] The pRep-Fluc expressed the Fluc protein. The pRep-BSD expressed the blasticidin S (BSD) resistance gene. pT7, T7 promoter; 5'UTR, HCV 5'-untranslated region; ΔC, truncated HCV core region (nt. 342–377); neo, neomycin phosphotransferase gene; EMCV, encephalomyocarditis virus; NS3, NS4, NS5A and NS5B, genes that encode HCV non-structural proteins; 3'UTR, HCV 3'-untranslated region.

HCV-directed siRNA *in vivo* may be effective in silencing viral protein expression in the liver. Here, we report that HCV replication was suppressed *in vitro* by recombinant retrovirus and adenovirus vectors expressing short hairpin RNA (shRNA) and that the delivery of the adenovirus vector to mice *in vivo* specifically inhibited viral protein synthesis in the liver.

Methods

Cells and cell culture

Huh7 and Retro Pack PT67 cells (Clontech, Palo Alto, CA, USA) were maintained in Dulbecco's modified minimal essential medium (Sigma, St. Louis, MO, USA) supplemented with 10% fetal calf serum at 37°C under 5% CO_2. To maintain cell lines carrying the HCV replicon, G418 (Wako, Osaka, Japan) was added to the culture medium to a final concentration of 500 μg/mL.

HCV replicon constructs and transfection

HCV replicon plasmids, pRep-Feo, pRep-Fluc and pRep-BSD were constructed from were constructed from a virus, HCV-N strain, genotype 1b.[21] The pRep-Feo expressed a chimeric reporter protein of firefly luciferase (Fluc) and neomycin phosphotransferase.[14,20] The pRep-Fluc and the pRep-BSD expressed the Fluc and blasticidin S (BSD) resistance genes, respectively (Fig. 1). The replicon RNA synthesis and the transfection protocol have been described previously.[22]

Synthetic siRNA and siRNA-expression plasmid

The design and construction of HCV-directed siRNA vectors have been described.[14] Briefly, five siRNA targeting the 5'-UTR of HCV RNA were tested for their efficiency to inhibit HCV replication, and the most effective sequence, which targeted nucleotide position of 331 though 351, was used in the present study. To construct shRNA-expressing DNA cassettes, oligonucleotide inserts were synthesized that contained the loop sequence (5'-TTC AAG AGA-3') flanked by sense and antisense siRNA sequences (Fig. 2a). These were inserted immediately downstream of the human U6 promoter. To avoid a problem in transcribing shRNA because of instability of the DNA strands arising from the tight palindrome structure, several C-to-T point mutations, which retained completely the silencing activity of the shRNA, were introduced into the sense strand of the shRNA sequences (referred to as 'm').[23] A control plasmid, pUC19-shRNA-Control, expressed shRNA directed towards the Machado–Joseph disease gene, which is a mutant of ataxin-3 gene and is not normally expressed. We have previously described the sequence specific activity of the shRNA-Control.[24]

Prior to construction of the virus vectors, we tested silencing efficiency of five shRNA constructs of different lengths that covered the target sequence (Fig. 2a). The shRNA-HCV-19, shRNA-HCV-21 and shRNA-HCV-27 had target sequences of 19, 21 and 27 nucleotides, respectively. Transfection of these shRNA constructs into Huh7/pRep-Feo showed that shRNA with longer target sequences had better suppressive effects (Fig. 2b). Therefore, we used shRNA-HCV-27m (abbreviated as shRNA-HCV) in the following study.

Recombinant retrovirus vectors

The U6-shRNA expression cassettes were inserted into the *StuI*/*Hin*dIII site of a retrovirus vector, pLNCX2 (Clontech) to construct pLNCshRNA-HCV and pLNCshRNA-Control (Fig. 2c). The plasmids were transfected into the packaging cells, Retro Pack PT67. The culture supernatant was filtered and added onto Huh7 cells with 4 μg/mL of polybrene. Huh7 cell lines stably expressing shRNA were established by culture in the presence of 500 μg/mL of G418.

Recombinant adenovirus

Recombinant adenoviruses expressing shRNA were constructed using an Adenovirus Expression Vector Kit (Takara, Otsu, Japan). The U6-shRNA expression DNA cassette was inserted into the *SwaI* site of pAxcw to construct pAxshRNA-HCV and pAxshRNA-Control. The adenoviruses were propagated according to the manufacturer's protocol (AxshRNA-HCV and AxshRNA-Control; Fig. 2c). A 'multiplicity of infection' (MOI) was used to standardize infecting doses of adenovirus. The MOI stands for the ratio of infectious virus particles to the number of cells being infected. An MOI = 1 represents equivalent dose to introduce one infectious virus particle to every host cell that is present in the culture.

Plasmids for assays of interferon responses

pISRE-TA-Luc (Invitrogen, Carlsbad, CA, USA) contained five copies of the consensus interferon stimulated response element (ISRE) motifs upstream of the Fluc gene. pTA-Luc (Invitrogen), which lacks the enhancer element, was used for background determination. The pcDNA3.1 (Invitrogen) was used as an empty vector for mock transfection. pRL-CMV (Promega, Madison, WI, USA), which expresses the *Renilla* luciferase protein, was used for normalization of transfection efficiency.[25] A plasmid, peGFPneo (Invitrogen), was used to monitor percentages of transduced cells.

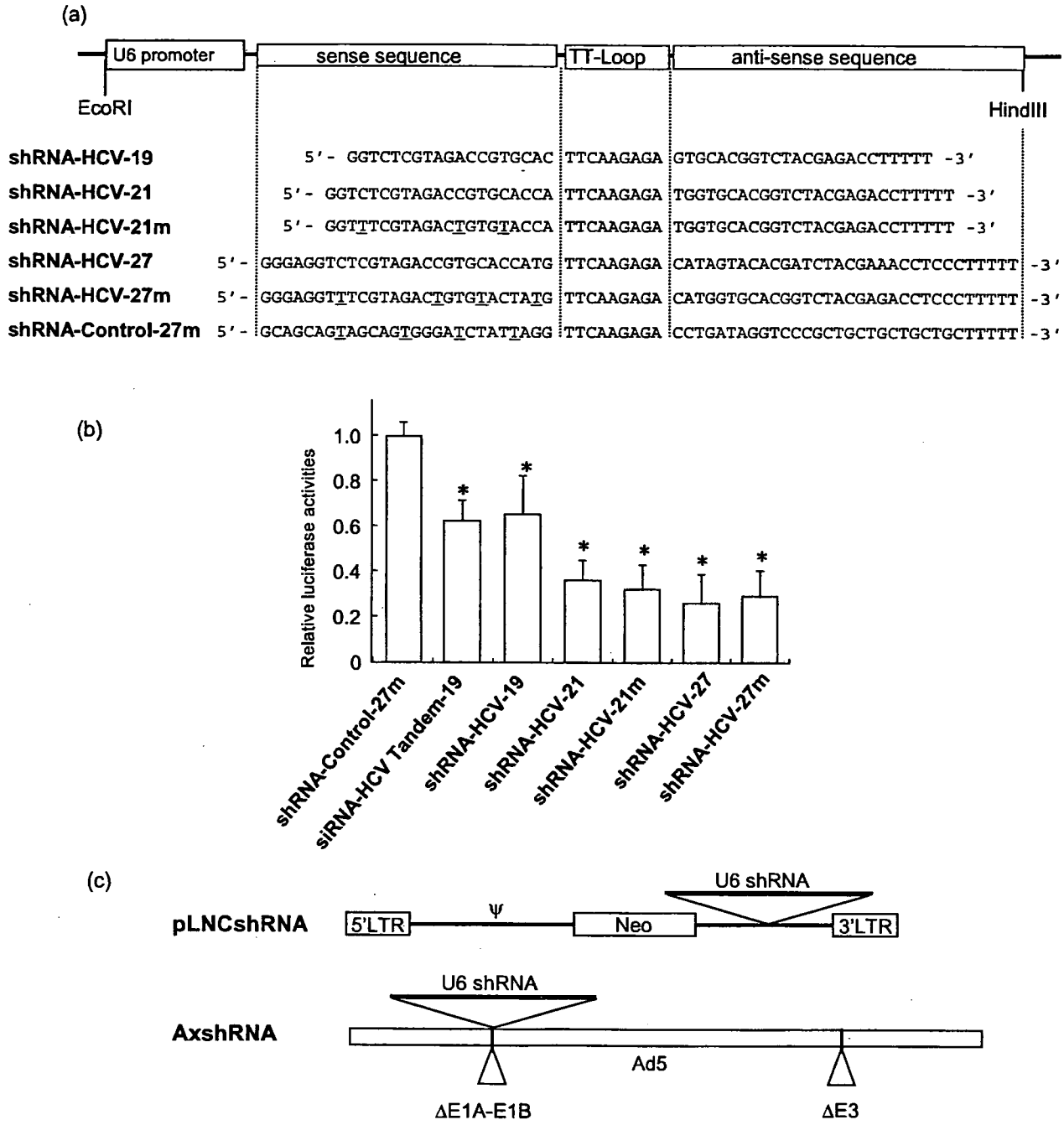

Figure 2 Structure of shRNA-expression constructs and shRNA sequences. (a) Structure of shRNA-expression cassette and shRNA sequences. TT-Loop, the loop sequence. The shRNA-Control was directed toward an unrelated target, Machado–Joseph disease gene. Underlined letters indicate C-to-T point mutations in the sense strand. (b) The shRNA-expression plasmids were transfected into Huh7/pRep-Feo cells, and internal luciferase activities were measured at 48 h of transfection. Each assay was done in triplicate, and the values are displayed as mean + SD. $^*P < 0.05$. (c) pLNCshRNA, structure of a recombinant retrovirus expressing shRNA. Ψ, the retroviral packaging signal sequence. AxshRNA, structure of a recombinant adenovirus expressing shRNA.

Real-time RT-PCR analysis

Total cellular RNA was extracted from cultured cells or liver tissue using ISOGEN (Nippon Gene, Tokyo, Japan). Total cellular RNA (2 μg) was used to generate cDNA from each sample using the SuperScript II reverse-transcriptase (Invitrogen). The mRNA expression levels were measured using the Light Cycler PCR and detection system (Roche, Mannheim, Germany) and Light Cycler Fast Start DNA Master SYBR Green 1 mix (Roche).

Luciferase assays

Luciferase activity was measured using a luminometer, Lumat LB9501 (Promega) and the Bright-Glo Luciferase Assay System (Promega) or the Dual-Luciferase Reporter Assay System (Promega).

Northern and western hybridization

Total cellular RNA was separated by denaturing agarose-formaldehyde gel electrophoresis, and transferred to a nylon membrane. The membrane was hybridized with a digoxigenin-labeled probe specific for the full-length replicon sequence, and subsequently with a probe specific for beta-actin. The signals were detected by chemiluminescence reaction using a Digoxigenin Luminescent Detection Kit (Roche), and visualized by Fluoro-Imager (Roche). For the western blotting, 10 μg of total cell lysate was separated on NuPAGE 4.12% Bis-TrisGel (Invitrogen), and blotted onto an Immobilon PVDF Membrane (Roche). The membrane was incubated with monoclonal antibodies specific for HCV-NS5A (BioDesign, Saco, ME, USA), NS4A (Virogen, Watertown, MA, USA), or beta-actin (Sigma), and detected by a chemiluminescence reaction (BM Chemiluminescence Blotting Substrate; POD, Roche).

Transient-replication assays

A replicon, pRep-Fluc, was transfected into cells and the luciferase activities of the cell lysates were measured serially. To correct the transfection efficiency, each value was divided by the luciferase activity at 4 h after the transfection.

Stable colony formation assays

Cells were transfected with a replicon, pRep-BSD, and were cultured in the presence of 150 μg/mL of BSD (Invitrogen). BSD-resistant cell colonies appeared after ~3 weeks of culture, and were counted.

HCV-JFH1 virus cell culture

An *in-vitro* transcribed HCV-JFH1 RNA[26] was transfected into Huh7.5.1 cells.[27] Naive Huh7.5.1 cells were subsequently infected by the culture supernatant of the JFH1-RNA transfected Huh-7.5.1 cells, and subjected to siRNA or drug treatments. Replication levels of HCV-RNA were quantified by the realtime RT-PCR by using primers that targeted HCV-NS5B region, HCV-JFH1 sense: 5′-TCA GAC AGA GCC TGA GTC CA-3′, and HCV-JFH1 antisense: 5′-AGT TGC TGG AGG GCT TCT GA-3′.

Mice and adenovirus infection

Transgenic mice, CN2-29, inducibly express mRNA for the HCV structural proteins (genotype1b, nucleotides 294–3435) by the Cre/*lox*P switching system.[28] The transgene does not contain full-length HCV 5′-UTR, but shares the target sequence of the shRNA-HCV. Although the transgenic mouse CN2 has been previously reported as expressing higher levels of the viral proteins, the expression levels of the viral core protein in the CN2-29 mice are modest and similar to that in the liver of HCV patients. Thus, we chose CN2-29 mice in the present study.

The mice were infected with AxshRNA-HCV or controls (AxshRNA-Control or AxCAw1) in combination with AxCAN-Cre, which expressed Cre recombinase. Three days after the infection, the mice were killed and HCV core protein in the liver was measured as described below. The BALB/c mice were maintained in the Animal Care Facility of Tokyo Medial and Dental University, and transgenic mice were in the Tokyo Metropolitan Institute of Medical Science. Animal care was in accordance with institutional guidelines. The review board of the university approved our experimental animal studies and all experiments were approved by the institutional animal study committees.

Measurement of HCV core protein in mouse liver

The amounts of HCV core protein in the liver tissue from the mice was measured by a fluorescence enzyme immunoassay (FEIA)[29] with a slight modification. Briefly, the 5F11 monoclonal anti-HCV-core antibody was used as the first antibody on the solid phase, and the 5E3 antibody conjugated with horseradish peroxidase was the second antibody. This FEIA can detect as little as 4 pg/mL of recombinant HCV-core protein. Contents of the HCV core protein in the liver samples were normalized by the total protein contents and expressed as pg/mg total protein.

Immunohistochemical staining

Liver tissue was frozen with optimal cutting temperature (OTC) compound (Tissue Tek; Sakura Finetechnical, Tokyo, Japan). The sections (8 μm thick) were fixed with a 1:1 solution of acetone : methanol at −20°C for 10 min and then washed with phosphate-buffered saline (PBS). Subsequently, the sections were incubated with the IgG fraction of an anti-HCV core rabbit polyclonal antibody (RR8)[28] in blocking buffer or antialbumin rabbit polyclonal antibody (Dako Cytomation, Glostrup, Denmark) in PBS overnight at 4°C. The sections were incubated with secondary antibody, Alexa-antirabbit IgG (Invitrogen) or TRITIC-antirabbit IgG (Sigma), for 2 h at room temperature. Fluorescence was observed using a fluorescence microscope.

Statistical analyses

Statistical analyses were performed using Student's *t*-test; *P*-values of less than 0.05 were considered to be statistically significant.

Results

Retrovirus transduction of shRNA can protect from HCV replication

Retrovirus vectors propagated from pLNCshRNA-HCV and pLNCshRNA-Control were used to infect Huh7 cells, and cell lines were established that constitutively express shRNA-HCV and shRNA-Control (Huh7/shRNA-HCV and Huh7/shRNA-Control, respectively). There were no differences in the cell morphology or growth rate between shRNA-transduced and non-transduced Huh7 cells (data not shown). The HCV replicon, pRep-Fluc, was transfected into Huh7/shRNA-HCV, Huh7/shRNA-Control and naive Huh7 cells by electroporation. In Huh7/shRNA-Control and naive Huh7 cells, the initial luciferase activity at 4 h decreased temporarily, which represents decay of the transfected replicon RNA, but increased again at 48 h and 72 h, which demonstrate de novo synthesis of the HCV replicon RNA. In contrast, transfection into Huh7/shRNA-HCV cells resulted in a decrease in the initial luciferase activity, reaching background by 72 h (Fig. 3a). Similarly, transfection of the replicon, pRep-BSD, into Huh7 cells and BSD selection yielded numerous BSD-resistant colonies in the naive Huh7 (832 colonies) and Huh7/shRNA-Control cell lines (740 colonies), while transfection of Huh7/shRNA-HCV, which expressed shRNA-HCV, yielded obviously fewer colonies (five colonies), indicating reduction of colony forming units by $\sim 10^2$ (Fig. 3b). There was no difference in shape, growth or viability between cells expressing the shRNA or not. These results indicated that cells expressing HCV-directed shRNA following retrovirus transduction acquired resistance to HCV replication.

Effect of recombinant adenoviruses expressing shRNA on *in vitro* HCV replication

We investigated subsequently the effects of recombinant adenovirus vectors expressing shRNA. AxshRNA-HCV and AxshRNA-Control were used separately to infect Huh7/pRep-Feo cells, and the internal luciferase activities were measured sequentially (Fig. 4a). AxshRNA-HCV caused continuous suppression of HCV RNA replication. Six days postinfection, the luciferase activities fell to background levels. In contrast, the luciferase activities of the Huh7/pRep-Feo cells infected with AxshRNA-Control did not show any significant changes compared with untreated Huh7/pRep-Feo cells (Fig. 4a). The dimethylthiazol carboxymethoxyphenyl sulfophenyl tetrazolium (MTS) assay showed no significant difference between cells that were infected by recombinant adenovirus and uninfected cells (Fig. 4b). In the northern blotting analysis, the cells were harvested 6 days after infection with the adenovirus at an MOI of 1. Feo-replicon RNA of 9.6 kb, which was detectable in the untreated Huh7/pRep-Feo cells and in the cells infected with AxshRNA-Control, diminished substantially following infection with the AxshRNA-HCV (Fig. 4c). Densitometries showed that the intracellular levels of the replicon RNA in the Huh7/pRep-Feo cells correlated well with the internal luciferase activities. Similarly in the western blotting, cells were harvested 6 days after infection with adenovirus. Levels of the HCV NS4A and NS5A proteins that were translated from the HCV replicon decreased following infection with the AxshRNA-HCV

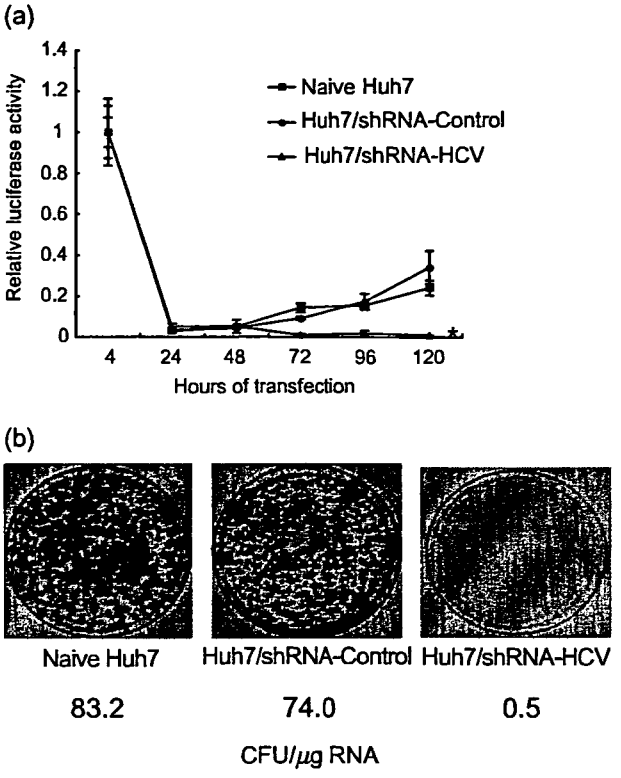

Figure 3 HCV replication can be inhibited by shRNA-HCV which was stably transfected into cells. Huh7/shRNA-HCV and Huh7/shRNA-Control stably express shRNA-HCV or shRNA-Control, respectively, following retroviral transduction. (a) Transient replication assay. An HCV replicon RNA, pRep-Fluc, was transfected into naive Huh7, Huh7/shRNA-HCV and Huh7/shRNA-Control cells. Luciferase activities of the cell lysates were measured serially at the times indicated, and the values were plotted as ratios relative to luciferase activities at 4 h. The luciferase activities at 4 h represent transfected replicon RNA. The data are mean ± SD. An asterisk denotes a *P*-value of less than 0.001 compared with the corresponding value of the naive Huh7 cells. (b) Stable colony formation assay. The HCV replicon, pRep-BSD, was transfected into naive Huh7, Huh7/shRNA-HCV and Huh7/shRNA-Control cells. The cells were cultured in the presence of blasticidin S (BSD) in the medium for ~3 weeks, and the BSD-resistant colonies were counted. These assays were repeated twice. The colony-forming units per microgram RNA (CFU/μg RNA) are shown at the bottom.

(Fig. 4d). These results indicated that the decrease in luciferase activities was due to specific suppressive effects of shRNA on expression of HCV genomic RNA and the viral proteins, and not due to non-specific effects caused by the delivery of shRNA or to toxicity of the adenovirus vectors.

Absence of interferon-stimulated gene responses by siRNA delivery

It has been reported that double-stranded RNA may induce interferon-stimulated gene (ISG) responses which cause instability of mRNA, translational suppression of proteins and apoptotic cell

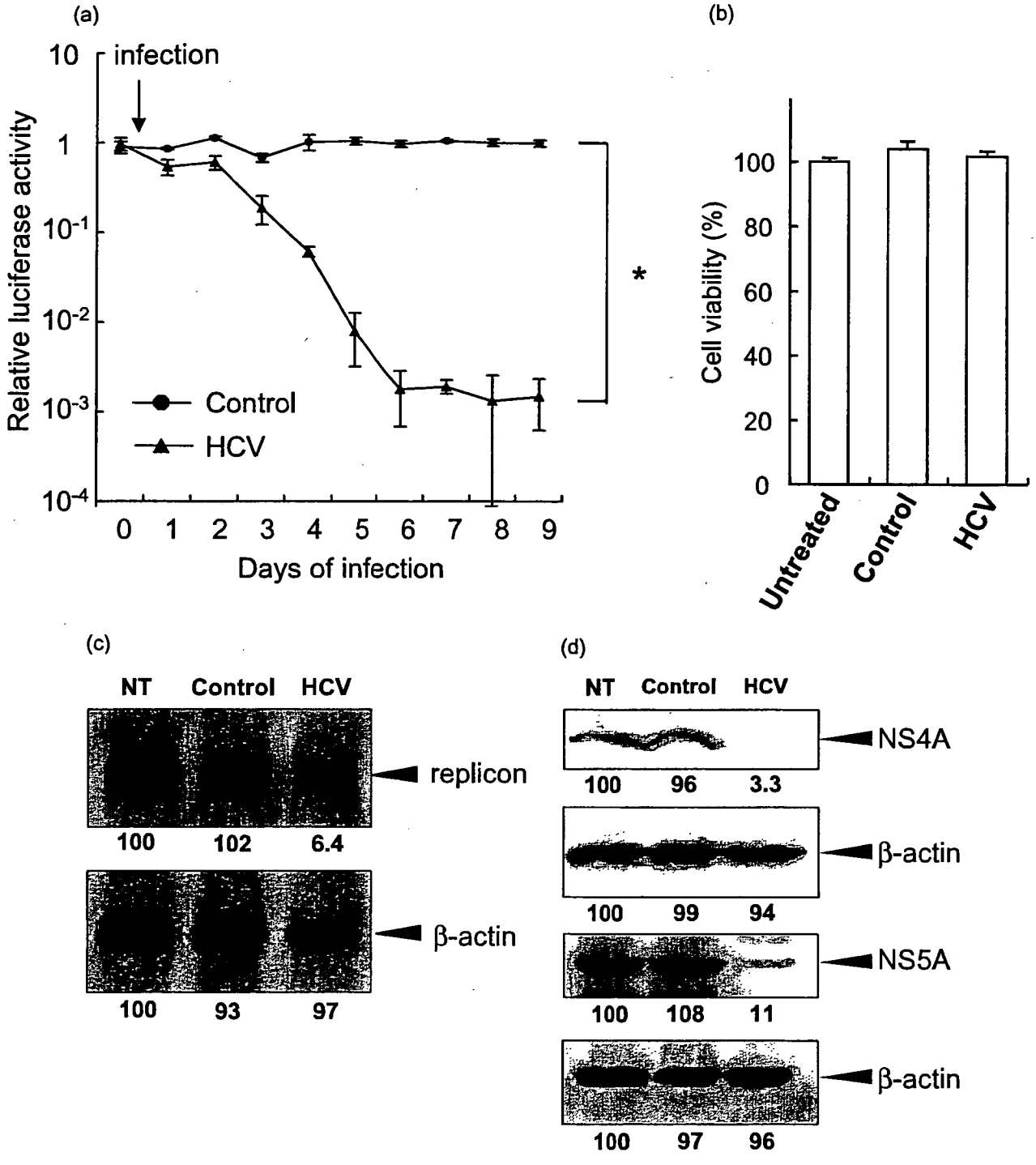

death.[18,30,31] Therefore, we examined the effects of the shRNA-expressing plasmids and adenoviruses on the activation of ISG expression in cells. The ISRE-reporter plasmid, pISRE-TA-Luc, and a control plasmid, peGFPneo, were transfected into Huh7 cells with plasmid pUC19-shRNA-HCV or pUC19-shRNA-Control, or adenovirus, AxshRNA-HCV or AxshRNA-Control, and the ISRE-mediated luciferase activities were measured. On day 2, the ISRE-luciferase activities did not significantly change in cells in which

Figure 4 Effect of a recombinant adenovirus expressing shRNA on HCV replicon. (a) Huh7/pRep-Feo cells were infected with AxshRNA-HCV or shRNA-Control at a multiplicity of infection (MOI) of 1. The cells were harvested, and internal luciferase activities were measured on day 0 though day 9 after adenovirus infection. Each assay was done in triplicate, and the value is displayed as a percentage of no treatment and as mean ± SD. An asterisk indicates a *P*-value of less than 0.05. (b) Dimethylthiazol carboxymethoxyphenyl sulfophenyl tetrazolium (MTS) assay of Huh7/pRep-Feo cells. Cells were infected with indicated recombinant adenoviruses at an MOI of 1. The assay was done at day 6 of infection. Error bars indicate mean + SD. (c) Northern blotting. The upper panel shows replicon RNA, and the lower panel shows beta-actin mRNA. (d) Western blotting. Total cell lysates were separated on NuPAGE gel, blotted and incubated with monoclonal anti-NS4A or anti-NS5A antibodies. The membrane was re-blotted with antibeta-actin antibodies. NT, untreated Huh7/pRep-Feo cells; Control, cells infected with AxshRNA-Control; HCV, cells treated with AxshRNA-HCV. In panels (b) and (c), cells were harvested on day 6 after adenovirus infection at an MOI of 1.

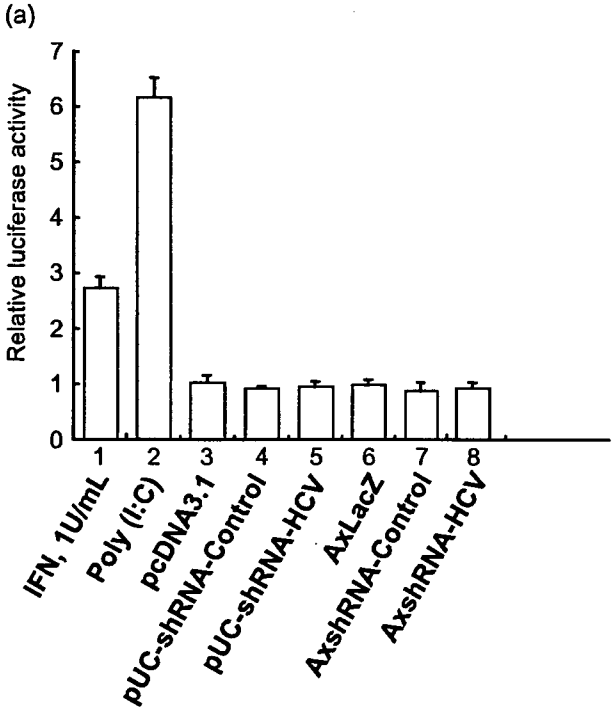

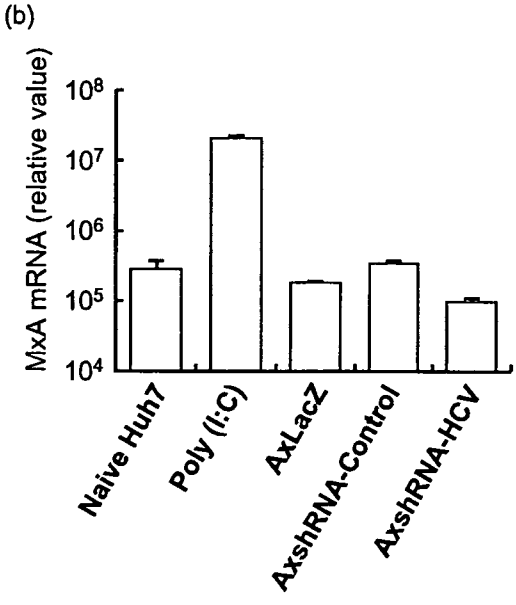

Figure 5 Interferon-stimulated gene responses by transfection of siRNA vectors. (a) Huh7 cells were seeded at 5×10^4 per well in 24-well plates on the day before transfection. As a positive control, 200 ng of pISRE-TA-Luc, or pTA-Luc, 1 ng of pRL-CMV, were transfected into a well using FuGENE-6 Transfection Reagent (Roche), and the cells were cultured with 1 U/mL of interferon (IFN) in the medium (lane 1). Lanes 3–5: 200 ng of pISRE-TA-Luc or pTA-Luc, and 1 ng of pRL-CMV were cotransfected with (lane2) 300 ng of poly (I : C), or 200 ng of plasmids (lane 3) pcDNA3.1, (lane 4) pUC19-shRNA-Control or (lane 5) pUC19-shRNA-HCV. Lanes 6–8: 200 ng of pISRE-TA-Luc or pTA-Luc, and 1 ng of pRL-CMV were transfected, and MOI = 1 of adenoviruses, (lane 6) AxLacZ, which expressed the beta-galactosidase (LacZ) gene under control of the chicken beta-actin (CAG) promoter as a control, (lane 7) AxshRNA-Control or (lane 8) AxshRNA-HCV were infected. Dual luciferase assays were performed at 48 h after transfection. The Fluc activity of each sample was normalized by the respective Rluc activity, and the respective pTA luciferase activity was subtracted from the pISRE luciferase activity. The experiment was done in triplicate, and the data are displayed as means + SD. (b) Huh7 cells were infected with indicated recombinant adenoviruses, AxLacZ, AxshRNA-Control and AxshRNA-HCV. RNA was extracted from each sample at day 6, and mRNA expression levels of an interferon-inducible MxA protein were quantified by the real-time RT-PCR analysis. Primers used were as follows: human MxA sense, 5′-CGA GGG AGA CAG GAC CAT CG-3′; human MxA antisense, 5′-TCT ATC AGG AAG AAC ATT TT-3′; human beta-actin sense, 5′-ACA ATG AAG ATC AAG ATC ATT GCT CCT CCT-3′; and human beta-actin antisense, 5′-TTT GCG GTG GAC GAT GGA GGG GCC GGA CTC-3′.

negative- or positive-control shRNA plasmids was transfected. (Fig. 5a). Similarly, the expression levels of an interferon-inducible MxA protein did not significantly change by transfection of shRNA-expression vectors (Fig. 5b). These results demonstrate that the shRNA used in the present study lack induction of the ISG responses both in the form of the expression plasmids and the adenovirus vectors.

Effect of siRNA and shRNA adenoviruses on HCV-JFH1 cell culture

The effects of HCV-targeted siRNA- and shRNA-expressing adenoviruses were confirmed by using HCV-JFH1 virus cell culture system. Transfection of the siRNA #331[14] into HCV-infected Huh7.5.1 cells resulted in substantial decrease of intracellular HCV RNA, while a control siRNA showed no effect (Fig. 6a). Similarly, infection of AxshRNA-HCV into Huh7.5.1/HCV-JFH1 cells specifically suppressed expression of HCV RNA (Fig. 6b).

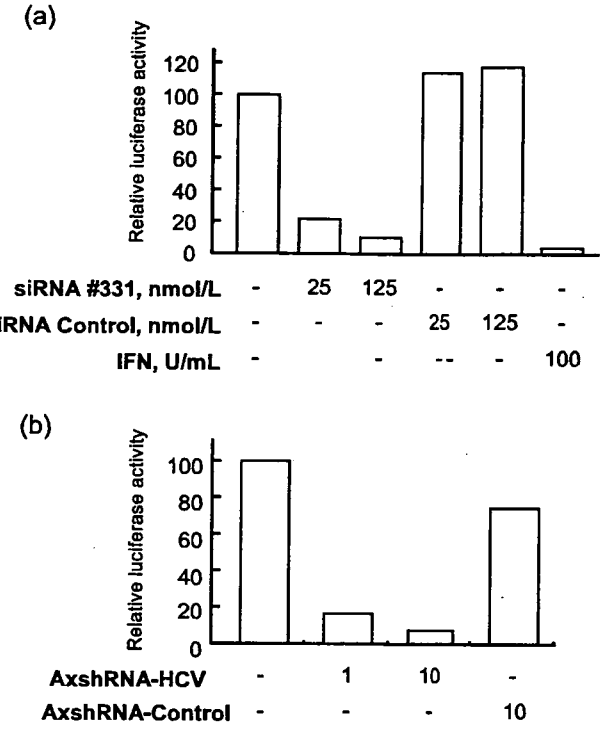

Figure 6 Effects of an siRNA and adenovirus expressing shRNA on HCV-JFH1 cell culture. (a) The siRNA #331, the siRNA-Control[14], (b) AxshRNA-HCV or AxshRNA-Control were, respectively, transfected or infected onto HV-JFH1-infected Huh7.5.1 cells. Seventy-two hours of the transfection or infection, expression level of HCV-RNA was quantified by real-time RT-PCR. The assays were repeated twice, and consistent results were obtained. IFN, recombinant interferon-alpha 2b.

Suppression of HCV-IRES-mediated translation *in vivo* by adenovirus expressing shRNA

The effects of the shRNA expression on the expression of the viral structural proteins *in vivo* were investigated using conditional HCV cDNA-transgenic mice, CN2-29.[28] Adenoviruses, AxshRNA-HCV, AxshRNA-Control or AxCAwl were injected into CN2-29 mice in combination with AxCANCre, an adenovirus expressing *Cre* DNA recombinase. The mice were killed on the fourth day after the injection, and the hepatic expression of the HCV core protein was measured. The expressed amounts of the core protein were 143.0 ± 56.2 pg/mg and 108.5 ± 42.4 pg/mg in AxCAwl and AxshRNA-Control-infected mice, respectively, and the expressed amount was significantly lower in mice injected with AxshRNA-HCV (28.7 ± 7.0 pg/mg, $P < 0.05$, Fig. 7a). Similarly, the induced expression of HCV core protein was not detectable by immunohistochemistry in AxshRNA-HCV infected liver tissue (Fig. 7c). Staining of a host cellular protein, albumin, was not obviously different between the liver infected with AxCAwl, AxshRNA-HCV and AxshRNA-Control (Fig. 7d). The expression levels of two ISG, IFN-beta and Mx1, in the liver tissue were not significantly different between individuals with and without injection of the adenovirus vectors (Fig. 7b). These results indicate specific shRNA silencing of HCV structural protein expression in the liver.

Discussion

The requirements to achieve a high efficiency using RNAi are: (i) selection of target sequences that are the most susceptible to RNAi; (ii) persistence of siRNA activity; and (iii) efficient *in vivo* delivery of siRNA to cells. We have used an shRNA sequence that was derived from a highly efficient siRNA (siRNA331), and constructed a DNA-based shRNA expression cassette that showed competitive effects with the synthetic siRNA (Fig. 2).[14] The shRNA-expression cassette does not only allow extended half-life of the RNAi, but also enables use of gene-delivery vectors, such as virus vectors. As shown in the results, a retrovirus vector expressing shRNA-HCV could stably transduce cells to express HCV-directed shRNA, and the cells acquired protection against HCV subgenomic replication (Fig. 3). An adenovirus vector expressing shRNA-HCV resulted in suppression of HCV subgenomic and protein expression by around three logs to almost background levels (Fig. 4). Consistent results were obtained by using an HCV cell culture (Fig. 6). More importantly, we have demonstrated *in-vivo* effects on viral protein expression in the liver using a conditional transgenic mouse model (Fig. 7). These results suggest that efficient delivery of siRNA could be effective against HCV infection *in vivo*.

An obstacle to applying siRNA technology to treat virus infections is that viruses are prone to mutate during their replication.[32] HCV continuously produces mutated viral strains to escape immune defense mechanisms. Even in a single patient, the circulating HCV population comprises a large number of closely related HCV sequence variants called quasispecies. Therefore, siRNA targeting the protein-coding sequence of the HCV genome, which have been reported by others,[15–19] may vary considerably among different HCV genotypes, and even among strains of the same genotype.[33] Our shRNA sequence targeted the 5′-UTR of HCV RNA, which is the most conserved region among various HCV isolates.[33] In addition, the structural constraints on the 5′-UTR, in terms of its requirement to direct internal ribosome entry and translation of viral proteins, might not permit the evolution of escape mutations. Our preliminary results have shown that the siRNA-HCV suppressed replication of an HCV genotype 2a replicon[34] to the same extent as the HCV 1b replicon.

Although the siRNA techniques rely on a high degree of specificity, several studies report siRNA-induced non-specific effect that may result from induction of ISG responses.[18,31] These effects may be mediated by activation of double-strand RNA-dependent protein kinase, toll-like receptor 3,[35] or possibly by a recently identified RNA helicase, RIG-I.[36] It remains to be determined whether these effects are generally induced by every siRNA construct. Sledz *et al.* have reported that transfection of two siRNA induced cellular interferon responses,[37] while Bridge *et al.* report that shRNA-expressing plasmids induced an interferon response but transfection of synthetic siRNA did not.[31] Speculatively, these effects on the interferon system might be construct dependent. Our shRNA-expression plasmids and adenoviruses did not activate ISG responses *in vitro* (Fig. 5a,b) or *in vivo* (Fig. 7b). We have preliminarily detected phosphorylated PKR (P-PKR) by western

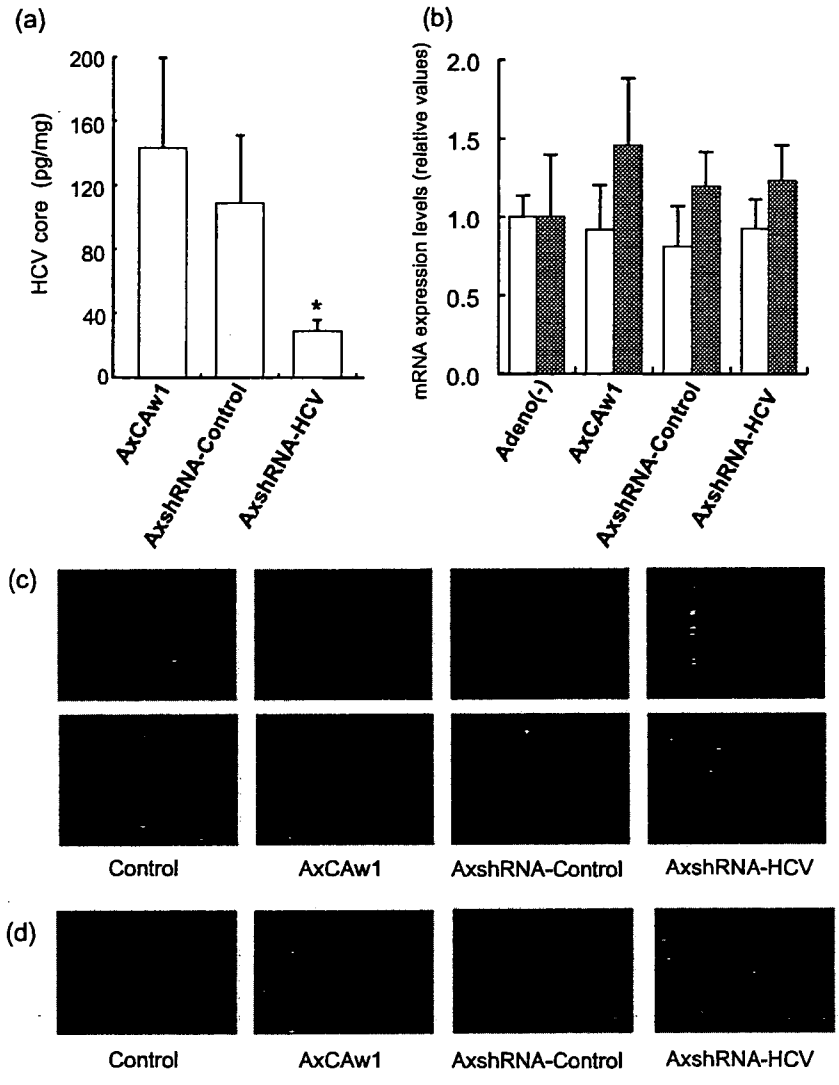

Figure 7 Effects of a recombinant adenovirus expressing shRNA on HCV core protein expression in CN2-29 transgenic mice. CN2-29 transgenic mice were administered with 1×10^9 PFU of AxCANCre combined with 6.7×10^8 PFU of AxshRNA-HCV, AxshRNA or AxCAw1. The mice were killed on day 4 after injection. (a) Quantification of HCV core protein in liver. Liver tissues were homogenized and used to determine the amount of HCV core protein. Each assay was done in triplicate, and the values are displayed as mean ± SD. Asterisk indicates *P*-value of less than 0.05. (b) Expression levels of mouse interferon-beta (white bars) and Mx1 (shaded bars) mRNA in the mouse liver tissue were quantified by the real-time RT-PCR analyses. Primers used were as follows: mouse interferon-beta sense, 5′-ACA GCC CTC TCC ATC AAC TA-3′; mouse interferon-beta antisense, 5′-CCC TCC AGT AAT AGC TCT TC-3′; mouse Mx1 sense, 5′-AGG AGT GGA GAG GCA AAG TC-3′; mouse Mx1 antisense, 5′-CAC ATT GCT GGG GAC TAC CA-3′; mouse beta-actin sense, 5′-ACT CCT ATG TGG GTG ACG AG-3′; mouse beta-actin antisense, 5′-ATA GCC CTC GTA GAT GGG CA-3′. Adeno (-) denotes mice without adenovirus administration. (c) Immunofluorescence microscopy of HCV core protein in the liver tissue. Liver sections of mice were stained using rabbit anticore polyclonal antibody and normal rabbit IgG as a negative control. The upper photographs were obtained at 400× magnification, and the lower photographs were at 1000×. (d) Immunofluorescence microscopy of albumin in liver. Liver sections from the mice were fixed and stained using rabbit antialbumin antibody and normal rabbit IgG as a negative control.

blotting, and found no apparent increase of P-PKR (data not shown). These results indicate that these target sequences and structures are of sufficient specificity to silence the target gene without eliciting non-specific interferon responses.

Beside the canonical action of siRNA, a sequence-specific cleavage of target mRNA, the siRNA could act as a micro-RNA that suppresses translational initiation of mRNA,[38] or it could mediate transcriptional gene silencing.[39] Regarding our *in-vivo* experiments, it was difficult to differentially analyze the effect of siRNA at individual sites of action because post-translational effect of siRNA concomitantly destabilizes target mRNA, which leads to apparent decrease of mRNA transcripts.

Efficiency and safety of gene transfer methods are the key determinants of the clinical success of gene therapy and an unresolved problem. There are several reports of delivery of siRNA or siRNA-expression vectors to cells *in vivo*;[12,40,41] however, gene delivery methods that are safe enough to apply to clinical therapeutics are currently under development. Adenovirus vectors are one of the most commonly used carriers for human gene therapies.[42–44] Our present results demonstrate that the adenoviral delivery of shRNA is effective in blocking HCV replication *in vitro* and virus protein expression *in vivo*. Adenovirus vectors have several advantages of efficient delivery of transgene both *in vitro* and *in vivo* and natural hepatotropism when administered *in vivo*. The AxshRNA-HCV specifically blocked expression of HCV structural proteins in a conditional transgenic mouse expressing those proteins. The current adenovirus vectors may cause inflammatory reactions in the target organ,[45] however, and produce neutralizing antibodies which make repeated administration difficult. These problems may be overcome by the improved constructs of virus vectors with attenuated immunogenicity or by the development of non-viral carriers for gene delivery.[46]

In conclusion, our results demonstrate the effectiveness and feasibility of the siRNA expression system. The efficiency of adenovirus expressing shRNA that target HCV suggests that delivery and expression of siRNA in hepatocytes may eliminate the virus and that this RNA-targeting approach might provide a potentially effective future therapeutic option for HCV infection.

Acknowledgments

This study was supported by grants from Japan Society for the Promotion of Science, 15590629 and 16590580, and partly supported by a grant from the Viral Hepatitis Research Foundation of Japan.

References

1 Alter MJ. Epidemiology of hepatitis C. *Hepatology* 1997; **26**: 62S–65S.
2 Hadziyannis SJ, Sette H Jr, Morgan TR *et al.* Peginterferon-alpha2a and ribavirin combination therapy in chronic hepatitis C: a randomized study of treatment duration and ribavirin dose. *Ann. Intern. Med.* 2004; **140**: 346–55.
3 Fire A, Xu S, Montgomery M, Kostas S, Driver S, Mello C. Potent and specific genetic interference by double-stranded RNA in Caenorhabditis elegans. *Nature* 1998; **19**: 806–11.
4 Elbashir SM, Harborth J, Lendeckel W, Yalcin A, Weber K, Tuschl T. Duplexes of 21-nucleotide RNAs mediate RNA interference in cultured mammalian cells. *Nature* 2001; **411**: 494–8.
5 Coburn GA, Cullen BR. Potent and specific inhibition of human immunodeficiency virus type 1 replication by RNA interference. *J. Virol.* 2002; **76**: 9225–31.
6 Jacque JM, Triques K, Stevenson M. Modulation of HIV-1 replication by RNA interference. *Nature* 2002; **418**: 435–8.
7 Gitlin L, Karelsky S, Andino R. Short interfering RNA confers intracellular antiviral immunity in human cells. *Nature* 2002; **418**: 430–4.
8 Ge Q, Filip L, Bai A, Nguyen T, Eisen HN, Chen J. Inhibition of influenza virus production in virus-infected mice by RNA interference. *Proc. Natl. Acad. Sci. USA* 2004; **101**: 8676–81.
9 Wang C, Pflugheber J, Sumpter R Jr *et al.* Alpha interferon induces distinct translational control programs to suppress hepatitis C virus RNA replication. *J. Virol.* 2003; **77**: 3898–912.
10 Klein C, Bock CT, Wedemeyer H *et al.* Inhibition of hepatitis B virus replication in vivo by nucleoside analogues and siRNA. *Gastroenterology* 2003; **125**: 9–18.
11 Konishi M, Wu CH, Wu GY. Inhibition of HBV replication by siRNA in a stable HBV-producing cell line. *Hepatology* 2003; **38**: 842–50.
12 McCaffrey AP, Meuse L, Pham TT, Conklin DS, Hannon GJ, Kay MA. RNA interference in adult mice. *Nature* 2002; **418**: 38–9.
13 Shlomai A, Shaul Y. Inhibition of hepatitis B virus expression and replication by RNA interference. *Hepatology* 2003; **37**: 764–70.
14 Yokota T, Sakamoto N, Enomoto N *et al.* Inhibition of intracellular hepatitis C virus replication by synthetic and vector-derived small interfering RNAs. *EMBO Rep.* 2003; **4**: 602–8.
15 Kapadia SB, Brideau-Andersen A, Chisari FV. Interference of hepatitis C virus RNA replication by short interfering RNAs. *Proc. Natl. Acad. Sci. USA* 2003; **100**: 2014–18.
16 Kronke J, Kittler R, Buchholz F *et al.* Alternative approaches for efficient inhibition of hepatitis C virus RNA replication by small interfering RNAs. *J. Virol.* 2004; **78**: 3436–46.
17 Randall G, Grakoui A, Rice CM. Clearance of replicating hepatitis C virus replicon RNAs in cell culture by small interfering RNAs. *Proc. Natl. Acad. Sci. USA* 2003; **100**: 235–40.
18 Seo MY, Abrignani S, Houghton M, Han JH. Letter to the editor: small interfering RNA-mediated inhibition of hepatitis C virus replication in the human hepatoma cell line Huh-7. *J. Virol.* 2003; **77**: 810–12.
19 Wilson JA, Jayasena S, Khvorova A *et al.* RNA interference blocks gene expression and RNA synthesis from hepatitis C replicons propagated in human liver cells. *Proc. Natl. Acad. Sci. USA* 2003; **100**: 2783–8.
20 Guo JT, Bichko VV, Seeger C. Effect of alpha interferon on the hepatitis C virus replicon. *J. Virol.* 2001; **75**: 8516–23.
21 Tanabe Y, Sakamoto N, Enomoto N *et al.* Synergistic inhibition of intracellular hepatitis C virus replication by combination of ribavirin and interferon-alpha. *J. Infect. Dis.* 2004; **189**: 1129–39.
22 Maekawa S, Enomoto N, Sakamoto N *et al.* Introduction of NS5A mutations enables subgenomic HCV-replicon derived from chimpanzee-infectious HC-J4 isolate to replicate efficiently in Huh-7 cells. *J. Viral. Hepat.* 2004; **11**: 394–403.
23 Miyagishi M, Sumimoto H, Miyoshi H, Kawakami Y, Taira K. Optimization of an siRNA-expression system with an improved hairpin and its significant suppressive effects in mammalian cells. *J. Gene Med.* 2004; **6**: 715–23.
24 Li Y, Yokota T, Matsumura R, Taira K, Mizusawa H. Sequence-dependent and independent inhibition specific for mutant ataxin-3 by small interfering RNA. *Ann. Neurol.* 2004; **56**: 124–9.
25 Kanazawa N, Kurosaki M, Sakamoto N *et al.* Regulation of hepatitis C virus replication by interferon regulatory factor-1. *J. Virol.* 2004; **78**: 9713–20.
26 Wakita T, Pietschmann T, Kato T *et al.* Production of infectious hepatitis C virus in tissue culture from a cloned viral genome. *Nat. Med.* 2005; **11**: 791–6.
27 Zhong J, Gastaminza P, Cheng G *et al.* Robust hepatitis C virus infection in vitro. *Proc. Natl. Acad. Sci. USA* 2005; **102**: 9294–9.
28 Wakita T, Taya C, Katsume A *et al.* Efficient conditional transgene expression in hepatitis C virus cDNA transgenic mice mediated by the Cre/loxP system. *J. Biol. Chem.* 1998; **273**: 9001–6.
29 Kashiwakuma T, Hasegawa A, Kajita T *et al.* Detection of hepatitis C virus specific core protein in serum of patients by a sensitive fluorescence enzyme immunoassay (FEIA). *J. Immunol. Methods* 1996; **28**: 79–89.

30 Baglioni C, Nilsen TW. Mechanisms of antiviral action of interferon. *Interferon* 1983; **5**: 23–42.
31 Bridge A, Pebernard S, Ducraux A, Nicoulaz A, Iggo R. Induction of an interferon response by RNAi vectors in mammalian cells. *Nat. Genet.* 2003; **34**: 263–4.
32 Carmichael GG. Silencing viruses with RNA. *Nature* 2002; **418**: 379–80.
33 Okamoto H, Okada S, Sugiyama Y *et al.* Nucleotide sequence of the genomic RNA of hepatitis C virus isolated from a human carrier: comparison with reported isolates for conserved and divergent regions. *J. Gen. Virol.* 1991; **72**: 2697–704.
34 Kato T, Date T, Miyamoto M *et al.* Efficient replication of the genotype 2a hepatitis C virus subgenomic replicon. *Gastroenterology* 2003; **125**: 1808–17.
35 Alexopoulou L, Holt AC, Medzhitov R, Flavell RA. Recognition of double-stranded RNA and activation of NF-kB by Toll-like receptor 3. *Nature* 2001; **413**: 732–8.
36 Yoneyama M, Kikuchi M, Natsukawa T *et al.* The RNA helicase RIG-I has an essential function in double-stranded RNA-induced innate antiviral responses. *Nat. Immunol.* 2004; **5**: 730–7.
37 Sledz C, Holko M, de Veer M, Silverman R, Williams, B. Activation of the interferon system by short-interfering RNAs. *Nat. Cell. Biol.* 2003; **5**: 834–9.
38 Doench JG, Petersen CP, Sharp PA. siRNAs can function as miRNAs. *Genes Dev.* 2003; **17**: 438–42.
39 Morris KV. siRNA-mediated transcriptional gene silencing: the potential mechanism and a possible role in the histone code. *Cell. Mol. Life Sci.* 2005; **62**: 3057–66.
40 Xia H, Mao Q, Paulson HL, Davidson BL. siRNA-mediated gene silencing in vitro and in vivo. *Nat. Biotechnol.* 2002; **20**: 1006–10.
41 Zender L, Hutker S, Liedtke C *et al.* Caspase 8 small interfering RNA prevents acute liver failure in mice. *Proc. Natl. Acad. Sci. USA* 2003; **100**: 7797–802.
42 Akli S, Caillaud C, Vigne E *et al.* Transfer of a foreign gene into the brain using adenovirus vectors. *Nat. Genet.* 1993; **3**: 224–8.
43 Bajocchi G, Feldman SH, Crystal RG, Mastrangeli A. Direct in vivo gene transfer to ependymal cells in the central nervous system using recombinant adenovirus vectors. *Nat. Genet.* 1993; **3**: 229–34.
44 Davidson BL, Allen ED, Kozarsky KF, Wilson JM, Roessler BJ. A model system for in vivo gene transfer into the central nervous system using an adenoviral vector. *Nat. Genet.* 1993; **3**: 219–23.
45 Yang Y, Wilson JM. Clearance of adenovirus-infected hepatocytes by MHC class I-restricted CD4+ CTLs in vivo. *J. Immunol.* 1995; **155**: 2564–70.
46 Fleury S, Driscoll R, Simeoni E *et al.* Helper-dependent adenovirus vectors devoid of all viral genes cause less myocardial inflammation compared with first-generation adenovirus vectors. *Basic Res. Cardiol.* 2004; **99**: 247–56.

Available online at www.sciencedirect.com
ScienceDirect
Life Sciences 81 (2007) 336–345
Life Sciences
www.elsevier.com/locate/lifescie

Tumor suppressor carcinoembryonic antigen-related cell adhesion molecule 1 potentates the anchorage-independent growth of human hepatoma HepG2 cells

Mariko Hokari [a], Yasunobu Matsuda [a,*], Toshifumi Wakai [b], Yoshio Shirai [b], Munehiro Sato [a], Atsunori Tsuchiya [a], Masaaki Takamura [a], Satoshi Yamagiwa [a], Kenji Suzuki [a], Shogo Ohkoshi [a], Takafumi Ichida [c], Hiroshi Kawachi [d], Yutaka Aoyagi [a]

[a] *Division of Gastroenterology and Hepatology, Niigata University Graduate School of Medical and Dental Sciences, Asahimachi-dori 1-757, Niigata 951-8510, Japan*
[b] *Division of Digestive and General Surgery, Niigata University Graduate School of Medical and Dental Sciences, Asahimachi-dori 1-757, Niigata 951-8510, Japan*
[c] *Department of Gastroenterology, Juntendo University Hospital of Shizuoka, Nagaoka 1129, Izu-nagaoka-cho, Tagata, Shizuoka 410-2295, Japan*
[d] *Department of Cell Biology, Institute of Nephrology, Niigata University Graduate School of Medical and Dental Sciences, Asahimachi-dori 1-757, Niigata 951-8510, Japan*

Received 9 March 2007; accepted 1 June 2007

Abstract

Carcinoembryonic antigen-related cell adhesion molecule 1 (CEACAM1), an adhesion molecule of the immunoglobulin superfamily, has been characterized as a putative tumor suppressor because it is frequently down-regulated in aggressive types of cancer cells. Recently, however, several studies have shown that CEACAM1 actively contributes to malignant progression or migration in some types of tumor cells, suggesting that the role of CEACAM1 might be diverse among different types of cancer cells. To investigate the functional consequences of CEACAM1 expression in hepatocellular carcinoma, we analyzed the status of CEACAM1 in hepatoma cell lines HLF, PLC/PRF/5, HepG2 and KYN-2. We found that CEACAM1 was only expressed in HepG2 cells, which show a unique property for enhanced anchorage-independent growth. When HepG2 cells were treated with small interfering RNA targeted against CEACAM1, the growth rate in monolayer culture was increased. In contrast, when HepG2 cells were cultured in suspension, inhibition of CEACAM1 expression significantly decreased the growth rate, and the speed of cell–cell attachment was repressed. Hyaluronidase treatment attenuated the growth rate of HepG2 cells in suspension culture, indicating that cell–cell attachment is a requisite for anchorage-independent growth. Our data may reveal the dual role of CEACAM1 on hepatocarcinogenesis, by showing that CEACAM1 acts as a tumor suppressor in HepG2 cells in anchorage-dependent growth conditions, while in anchorage-independent growth conditions, it augments cell proliferation by potentiating the cell–cell attachment.

Keywords: CEACAM1; HepG2; Anchorage-independent growth; Small interfering RNA

Introduction

Carcinoembryonic antigen-related cell adhesion molecule 1 (CEACAM1), also known as biliary glycoprotein (BGP), CD66a and pp120, is a member of the carcinoembryonic antigen family of immunoglobulin-like adhesion molecules. CEACAM1 has generally been considered to be a tumor suppressor based on decreased expression in cancer cells including breast (Obrink, 1997; Riethdorf et al., 1997), colorectal (Neumaier et al., 1993; Brummer et al., 1995), prostate (Kleinerman et al., 1995; Luo et al., 1999), bladder (Kleinerman et al., 1996) and endometrial carcinoma (Bamberger et al., 1998). As it has been reported that forced expression of CEACAM1 reduced tumorigenesis in prostate and colon cancer cells (Hsieh et al., 1995; Kunath et al., 1995; Luo et al., 1999; Busch et al., 2002),

* Corresponding author. Tel.: +81 25 227 2207; fax: +81 25 227 0776.
E-mail address: yasunobu@med.niigata-u.ac.jp (Y. Matsuda).

0024-3205/$ - see front matter © 2007 Elsevier Inc. All rights reserved.
doi:10.1016/j.lfs.2007.06.002

CEACAM1 may play an important role in preventing carcinogenesis, together with many other cell–cell adhesion molecules.

Recently, however, several studies have revealed that CEACAM1 actively contributes to the malignant progression in some types of cancer cells. Overexpression of CEACAM1 has been found in melanoma (Brummer et al., 2001; Thies et al., 2002), gastric cancer (Kinugasa et al., 1998) and non-small cell lung cancer (Laack et al., 2002; Sienel et al., 2003) where the cancer is invasive or in individuals with poorer prognosis. More significantly, it has recently been shown that CEACAM1 expression markedly enhanced cell invasion and migration of melanoma cells (Ebrahimnejad et al., 2004) and thyroid cancer cells (Liu et al., 2006). These lines of evidence strongly indicate that the biological behavior of CEACAM1 may be different among different types of cancer cells.

Hepatocellular carcinoma (HCC) is one of the most aggressive malignancies worldwide, and often metastasizes to non-cancerous liver tissue. In general, cancer metastasis is governed by a multi-

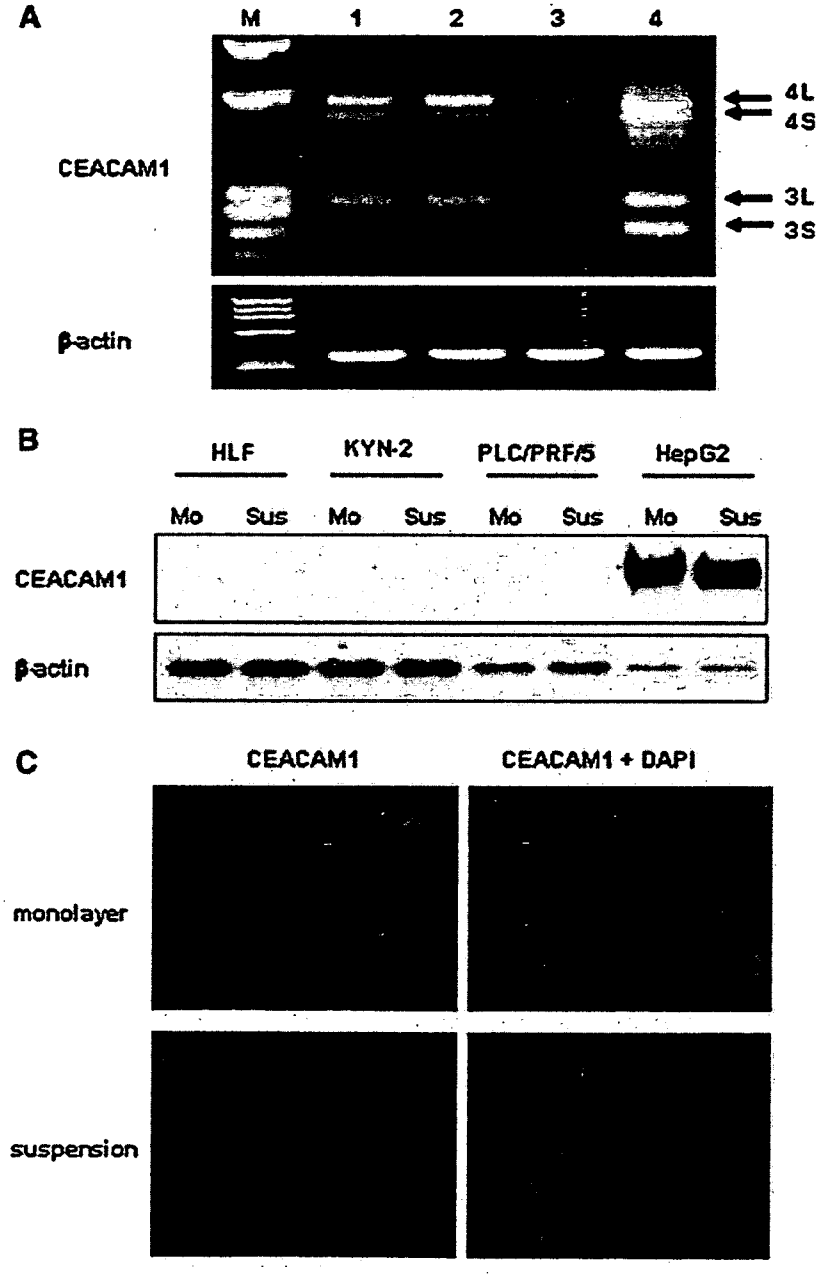

Fig. 1. Expression of CEACAM1 in hepatoma cells. (A) Reverse transcription — polymerase chain reaction analysis of CEACAM1 gene. Total RNA was extracted from hepatoma cells in monolayer culture after 48 h. The CEACAM1 gene was reverse-transcribed and amplified, and β-actin mRNA was used as the internal control. Arrows indicate PCR bands corresponding to mRNAs of CEACAM1-3S (3S: 243 bp), CEACAM1-3L (3L: 296 bp), CEACAM1-4S (4S: 531 bp) and CEACAM1-4L (4L: 584 bp). M, ΦX174 DNA/Hae III; 1, HLF; 2, KYN-2; 3, PLC/PRF/5; 4, HepG2 cells. (B) Immunoblotting analysis of CEACAM1 protein expression. Mo, monolayer culture; Sus, suspension culture. (C) Immunofluorescence staining for CEACAM1 in HepG2 cells in monolayer culture (upper panel) and suspension culture (lower panel) after 48 h. Left, immunostaining for CEACAM1 (red); right, merged images of CEACAM1 immunostaining (red) and DAPI (blue). (magnifications: ×40).

step process comprising (1) detachment of cancer cells from the tumor periphery, (2) entry from the stroma into the vascular system, (3) anchorage-independent growth while circulating in the blood stream, and (4) cell proliferation at the seeded site. Increased ability for anchorage-independent growth may significantly affect the metastatic potential of HCC, because the number of viable cancer cells circulating in the blood stream may determine the number of metastatic foci in the liver or distal organs. To date, many studies have suggested that CEACAM1 exerts an inhibitory effect during the progression of HCC. CEACAM1 expression was found to be decreased in HCC compared with adjacent non-cancerous regions (Tanaka et al., 1997), and the loss of CEACAM1 expression adversely affected the survival of individuals with HCC (Cruz et al., 2005). Moreover, restoration of CEACAM1 expression in rat HCC cells suppressed tumorigenesis in vivo (Laurie et al., 2005), indicating that CEACAM1 is a putative tumor suppressor in HCC. However, considering the diverse role of CEACAM1 among different types of cancer cells, it is still unclear whether CEACAM1 acts only as a tumor suppressor, including during the process of HCC metastasis.

In this study, we found that the biological potential of CEACAM1 was significantly different between cultured hepatoma HepG2 cells with and without anchorage dependence. When HepG2 cells were cultured in monolayer, CEACAM1 exerted an inhibitory effect on cell proliferation. When HepG2 cells were cultured in anchorage-independent growth conditions, however, treatment with small interfering RNA targeting CEACAM1 repressed the growth rate. Our results show a dual role of CEACAM1 on hepatoma cells and suggest that this adhesion molecule should not be considered a simple tumor suppressor in HCC.

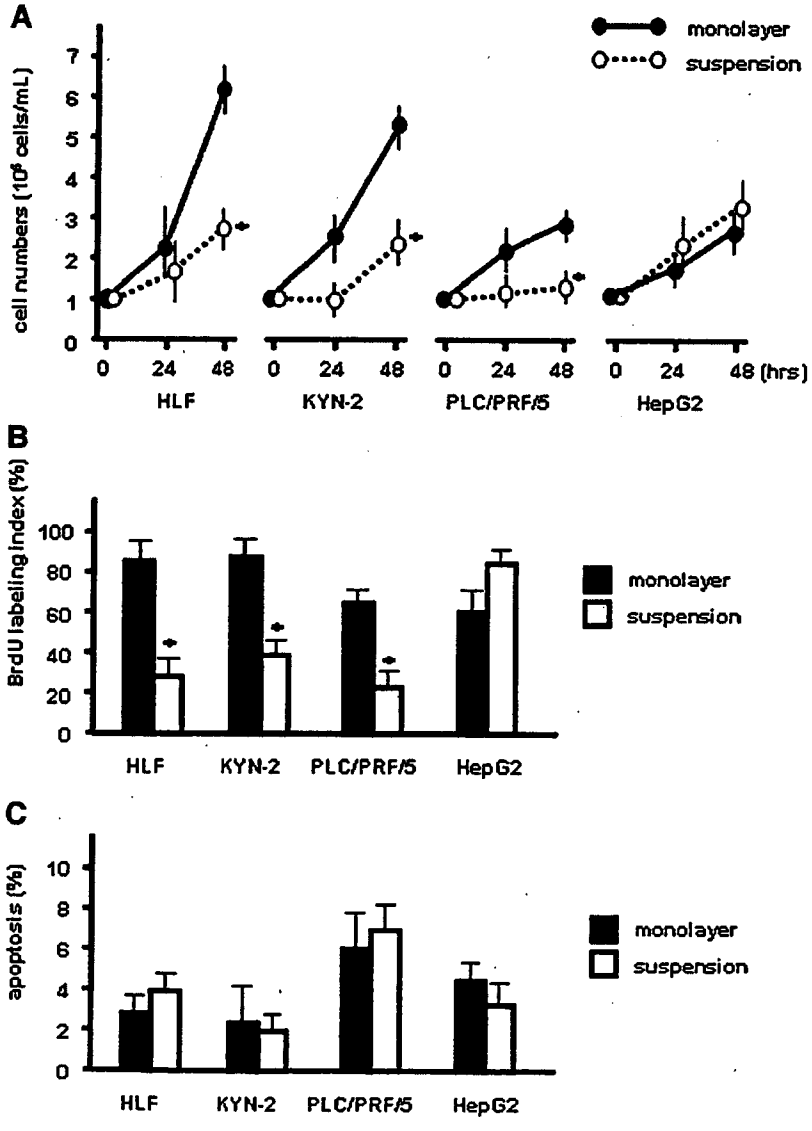

Fig. 2. Proliferation of hepatoma cells in monolayer and suspension culture. (A) Growth curve of hepatoma cells. Cells (1×10^5 cells/mL) were cultured in monolayer or suspension, and cell numbers were determined at the indicated time intervals. Values shown are the mean of triplicate dishes. Points, mean; bars, standard deviation (S.D.). (B) BrdU labeling index of hepatoma cells in monolayer and suspension culture after 48 h. (C) Percentage of TUNEL-positive apoptotic cells in monolayer and suspension culture after 48 h. Filled column, monolayer; open column, suspension; bars, S.D.; $^*p<0.05$.

Materials and methods

Materials

Dulbecco's modified Eagle's medium (DMEM), RPMI-60 medium, and fetal bovine serum were obtained from Invitrogen (Carlsbad, CA, USA). Polyhydroxyethylmethacrylate (poly-HEMA) and hyaluronidase were obtained from Sigma Chemical (St Louis, MO, USA). For immunoblotting, anti-CEACAM1 mouse monoclonal antibody (283340) was obtained from R&D systems (Minneapolis, MN, USA) and antibody for actin was obtained from Chemicon (Temecula, CA, USA).

Cell lines and culture

Human hepatoma cell lines HLF, PLC/PRF/5 and HepG2 (Riken Cell Bank, Tsukuba, Japan) were cultured in DMEM medium, and KYN-2 cells (kindly provided by Dr M Kojiro, Kurume University, Kurume, Japan) (Yano et al., 1988) were cultured in RPMI-60 medium. Culture media were supplemented with 100 U/ml penicillin, 100 mg/ml streptomycin and 10% fetal bovine serum. Cells (1×10^5 cells/mL) were cultured in monolayer on the culture dishes, or in suspension by plating on poly-HEMA (a nonionic material that blocks cell attachment) coated culture dishes at 37 °C in an incubator containing 5% CO_2. In the cell-aggregation assay (Tanaka et al., 1997), single cell suspensions (1×10^5 cells/mL) were made by passing trypsinized cells through a 27-gauge needle three times, then seeded on a poly-HEMA-coated dish and shaken at 70 rpm for 2 h. To disrupt cell aggregation, 2 mg/ml hyaluronidase was added to the suspension culture (Mueller et al., 2000).

Proliferation and apoptosis assays

Cells (1×10^5/mL) in monolayer or suspension culture were harvested at the times indicated. They were trypsinized, dispensed as either single cells or small clumps by differential cycles of mechanical aspiration, and counted by microscopic analysis (Zhang et al., 2006). The percentage of cells in the S-phase was determined by measuring incorporation of 5-bromo-2′-deoxyuridine (BrdU). Briefly, 40 μM BrdU was added to the culture media 24 h before the cells were fixed in cold ethanol, and mouse anti-BrdU antibody (DAKO A/S; Copenhagen, Denmark) was used as the primary antibody. BrdU staining was visualized by using the Vectastain Elite ABC kit (Vector; Burlingame, CA, USA) and labeled cells were counted. Apoptotic cell death was evaluated by TUNEL (Terminal deoxynucleotidyl Transferase Biotin-dUTP Nick End Labeling) using ApopTag Plus Peroxidase *In Situ* Apoptosis Detection Kit (Millipore; Bedford, MA, USA). For statistical analysis, three lots of 100 cells were counted in five random microscopic fields at ×400 magnification.

Immunoblotting

In all experiments, levels of CEACAM1 expression were analyzed after 48 h of culture. Protein samples were extracted in lysis buffer (50 mM Tris pH 8.0, 150 mM sodium chloride, 1 mM sodium vanadate, 0.1% (v/v) sodium dodecyl sulfate (SDS), and 1% Nonidet P-40) and precleared by centrifugation, and the concentration was determined using a Bradford assay (Bio-Rad Laboratories, Hercules, CA, USA). Samples (10 μg) were electrophoresed on SDS-polyacrylamide gels and transferred to Immobilon membranes (Millipore). After blocking nonspecific sites, filters were reacted with primary antibodies and corresponding horseradish peroxidase-conjugated secondary antibodies. Protein bands were visualized using an enhanced chemiluminescence detection system (GE Healthcare Bio-Sciences; Tokyo, Japan).

Immunofluorescence staining

Cells were fixed with 4% paraformaldehyde in phosphate buffered saline (PBS) (pH 7.4) and permeabilized with 0.1% Triton X-100. Fixed cells were incubated with 2% swine serum, reacted with anti-CEACAM1 monoclonal antibody (29H2; 1:500) (Novocastra Laboratories; Newcastle upon Tyne, UK) at 4 °C overnight, and incubated with the Alexa Fluor 546-labeled anti-mouse goat IgG (Invitrogen). Actin filaments were visualized using Alexa Fluor 488-labeled phalloidin (Invitrogen). Stained cells were mounted with 4′,6-diamidino-2-phenylindole (DAPI) (Vector) and examined using an Axio Imager A1 microscope (Carl Zeiss).

Reverse transcription-polymerase chain reaction

Total RNA was prepared using the RNeasy Kit (Qiagen, Hilden, Germany) and subjected to reverse transcription using the

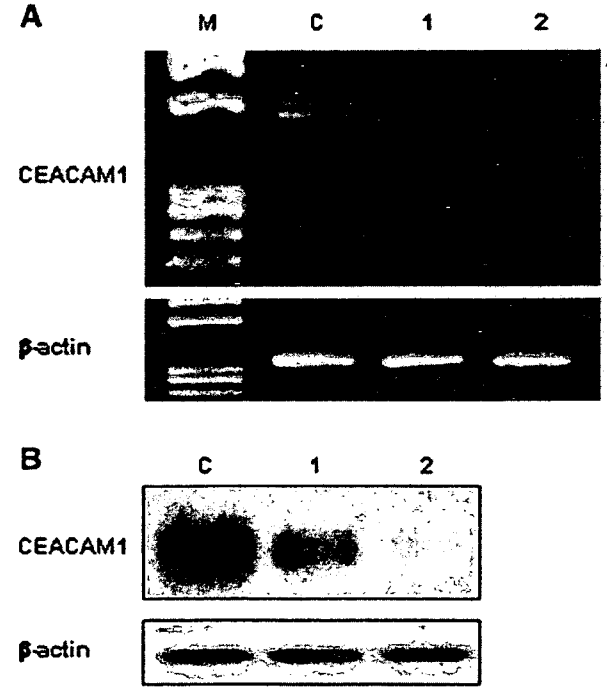

Fig. 3. Effect of siRNA on CEACAM1 expression. (A) RT-PCR analysis of CEACAM1 mRNA in HepG2 cells treated with siRNA for 24 h. Cycling conditions: 23 cycles for CEACAM1 gene and 20 cycles for β-actin gene. (B) Western blotting analysis of HepG2 cells treated with siRNA for 48 h. M, ΦX174 DNA/Hae III; (C) Cells treated with control siRNA. 1, Cells treated with CEACAM1 siRNA#1; 2, Cells treated with CEACAM1 siRNA#2.

First Strand cDNA Synthesis Kit for RT-PCR (AMV) (Roche Diagnostics; Mannheim, Germany). Reverse transcription-polymerase chain reaction (RT-PCR) was performed using *Taq*Bead Hot Start Polymerase (Promega; Mannheim, Germany). PCR conditions were 35 cycles of denaturation, annealing, and extension (94 °C for 1 min, 55 °C for 2 min and 72 °C for 3 min). DNA primers for the human CEACAM1 gene were sense 5′-CTG CAA CAG GAC CAC AGT CAA G-3′ and anti-sense 5′-GCT GGG CTT CAA AGT TCA GGG T-3′, which encompass from the extracellular B1 domain to the cytoplasmic domain and can amplify four alternatively spliced mRNA transcripts of CEACAM1 (CEACAM1-3L, 3S, 4L and 4S) (Takahashi et al., 1993). Human β-actin primers were sense 5′-GGT CAC CCA CAC TGT GCC CAT-3′ and anti-sense 5′-GGA TGC CAC AGG ACT CCA TGC-3′ (generating a 350-bp fragment) (McCaffrey et al., 2000). The PCR products were visualized by electrophoresis on an agarose gel stained with ethidium bromide, and the intensity of the bands was quantified by densitometry.

RNA interference

Small interfering RNA (siRNA) duplexes designed to target CEACAM1 were synthesized by Sigma Genosys (Woodlands, TX, USA) as follows: 5′-UAG UGG AUC CUA UAC CUG CCA-3′ (sense) and 5′-GCA GGU AUA GGA UCC ACU ACA-3′ (antisense) (siRNA#1), and 5′-UAA CUC AGU CAC UGG CUG CAA-3′ (sense), 5′-GCA GCC AGU GAC UGA GUU AAA-3′ (antisense) (siRNA#2). All siRNAs were evaluated for sequence specificity by a siDirect™ search (Naito et al., 2004) and did not show homology to other known genes. Negative Control siRNA (Ambion) was used as a control oligo. Transfection of cells was carried out using the siPORT *Neo*FX transfection protocol (Ambion Inc.; Austin, TX, USA) according to the manufacturer's instructions. Briefly, siPORT *Neo*FX (Ambion) was incubated in Opti-MEM medium (Invitrogen) for 10 min. The siRNA oligo or control oligo was diluted in Opti-MEM medium to give a final concentration of 100 nM, and mixed 1:1 with the siPORT *Neo*FX for a further 10 min

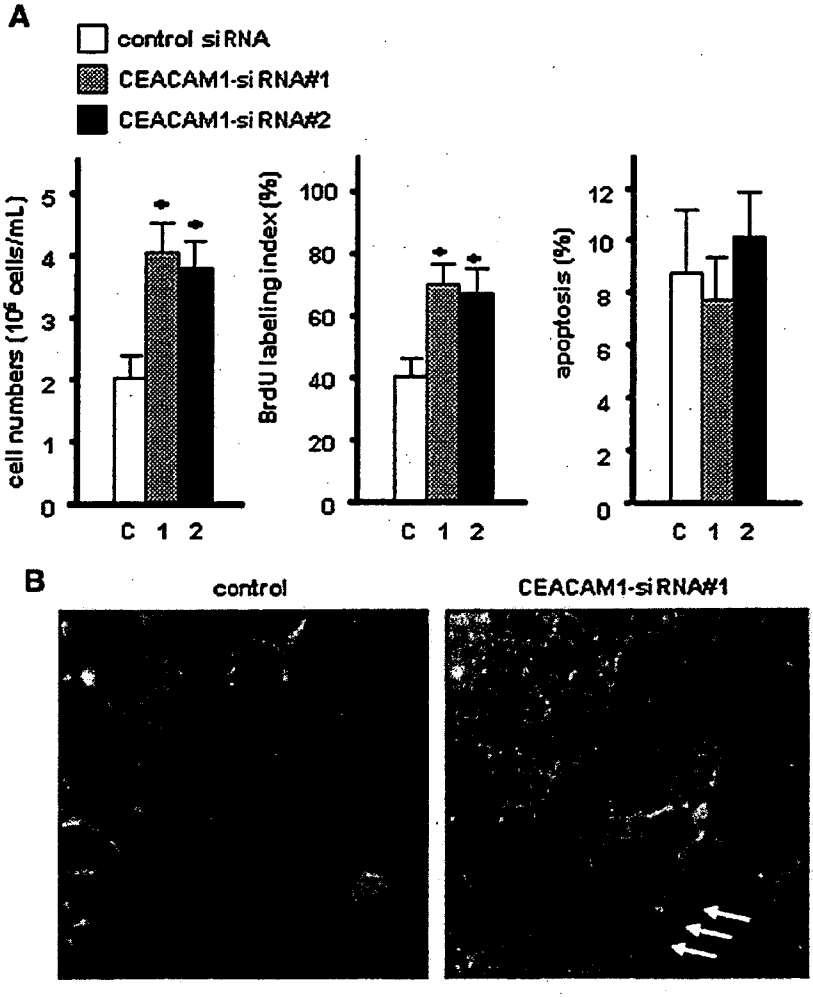

Fig. 4. Effect of CEACAM1 siRNA on HepG2 cells in monolayer culture. (A) Cells were treated as described in "Materials and methods" section, and were analyzed according to cell numbers, BrdU labeling indices and TUNEL-positive cells. (C) Control siRNA-treated cells; 1, CEACAM1-siRNA#1-treated cells; 2, CEACAM1-siRNA#2-treated cells; bars, S.D.; *$p<0.05$ vs. control. (B) Alexa Fluor 488-labeled actin filaments of HepG2 cells treated with control siRNA (control) and CEACAM1-siRNA#1 (CEACAM1-siRNA#1). arrows, ruffled cell membranes (magnifications: × 40).

incubation. The mixture (200 μL) was placed in each well of a 6-well plate and overlaid with 1×10^5 cells/ml (2.3 mL) in normal growth medium. Cells were trypsinized 48 h after transfection, and cultured on a dish plate with or without poly-HEMA at a density of 1×10^5 cells/mL for 48 h.

Statistical analysis

The results are presented as mean±SD. The student's *t*-test was used for statistical evaluation, and $P<.05$ was considered significant.

Results

Expression of CEACAM1 in hepatoma cells

RT-PCR analysis detected the splicing variants of CEACAM1 mRNAs in all hepatoma cells, with predominant expression of CEACAM1-3L and CEACAM1-4L mRNA transcripts. HepG2 cells showed the strongest expression of all mRNAs, ranging from 8 to 30 times the expression in the other cells (Fig. 1A). Immunoblotting showed that CEACAM1 protein was only expressed in HepG2 cells, and the level of protein expression was almost the same in monolayer and suspension cultures (Fig. 1B). Immunofluorescence staining detected highly concentrated CEACAM1 expression at the lateral cell–cell contact area of HepG2 cells in monolayer culture (Fig. 1C), while for cells in suspension, lateral staining for CEACAM1 was reduced and diffuse expression was observed on the cell bodies.

Proliferation of hepatoma cells in monolayer and suspension culture

For HLF, KYN-2 and PLC/PRF/5 cells, growth rate in suspension culture was significantly decreased when compared

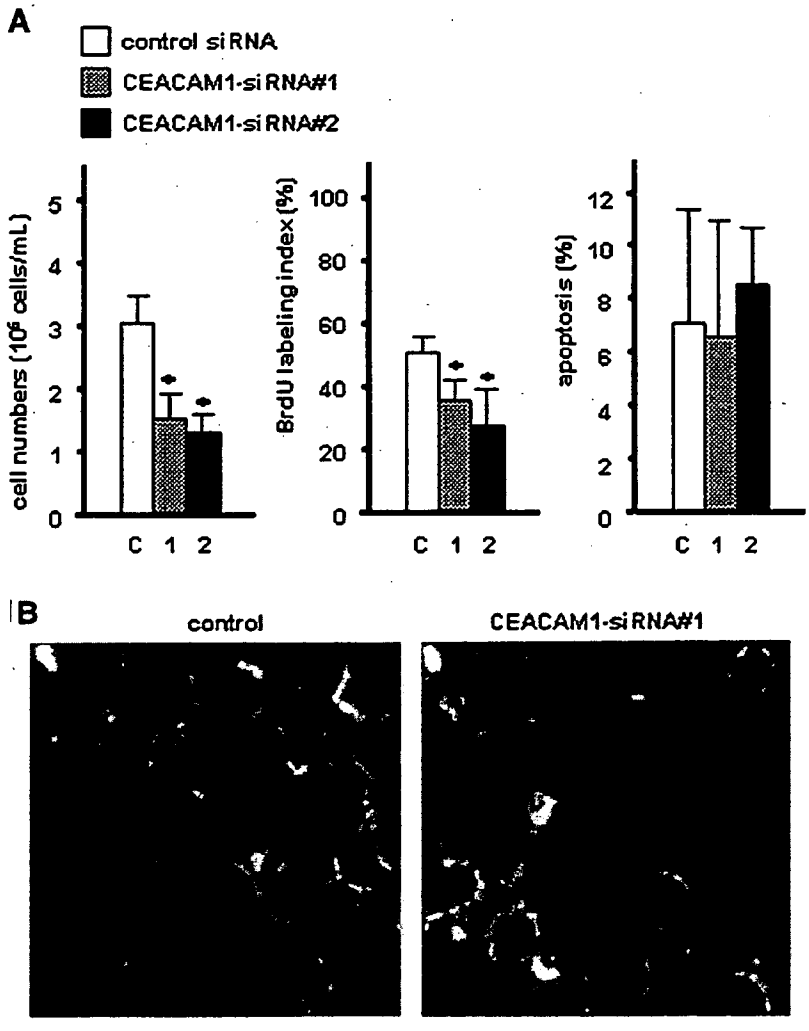

Fig. 5. Effect of CEACAM1 siRNA on HepG2 cells in suspension culture. (A) Cells were treated as described in "Materials and methods" section, and were analyzed according to cell numbers, BrdU labeling indices and TUNEL-positive cells. (C) Control siRNA-treated cells; 1, CEACAM1-siRNA#1-treated cells; 2, CEACAM1-siRNA#2-treated cells; bars, S.D.; <0.05 vs. control. (B) Alexa Fluor 488-labeled actin filaments of HepG2 cells treated with control siRNA (control) and CEACAM1-siRNA#1 (CEACAM1-siRNA#1) (magnifications: ×40).

with monolayer culture (monolayer *vs* suspension; HLF, 6.1±0.5 *vs.* 2.6±0.3×10^5 cells/mL, $p<0.05$; KYN-2, 5.2±0.4 *vs.* 2.2±0.4×10^5 cells/mL, $p<0.05$; PLC/PRF/5, 2.6±0.2 *vs.* 1.1±0.3×10^5 cells/mL, $p<0.05$). In contrast, growth rate of HepG2 cells in suspension culture was almost the same as in monolayer culture (monolayer *vs.* suspension; 2.3±0.5 *vs.* 2.8±0.4×10^5 cells/mL, $p=0.21$) (Fig. 2A). BrdU labeling indices of HLF, KYN-2 and PLC/PRF/5 cells were significantly lower in suspension culture than in monolayer culture ($p<0.05$), whereas the labeling index of HepG2 cells was relatively higher in suspension than in monolayer (monolayer *vs.* suspension, 64±10% *vs.* 82±7%, $p=0.06$) (Fig. 2B). No significant difference was observed in the ratio of apoptotic cells between monolayer and suspension cultures in any cell lines (Fig. 2C).

siRNA-mediated silencing of CEACAM1 in HepG2 cells in monolayer culture

To investigate whether strong CEACAM1 expression is associated with enforced anchorage-independent growth of HepG2 cells, the effect of siRNA targeting of CEACAM1 on growth rate was examined. CEACAM1 siRNA-treated cells showed significant reduction of all splicing variants of mRNAs (Fig. 3A). Immunoblotting analysis confirmed that the level of CEACAM1 protein in siRNA-treated cells was less than 20% of that in mock transfectants (Fig. 3B). When CEACAM1 siRNA-transfected HepG2 cells were cultured in monolayer for 48 h, cell proliferation was increased compared with mock transfectants (siRNA#1 *vs.* siRNA#2 *vs.* mock; 4.0±0.5, 3.7±0.3, 2.0±0.4×10^4 cells/mL; $p<0.05$, $p<0.05$ compared with mock transfectants) (Fig. 4A). CEACAM1 siRNA-transfected cells showed a higher BrdU labeling index compared with mock transfectants (siRNA#1 *vs.* siRNA#2 *vs.* mock; 72±6%, 66±6%, 40±5%; $p<0.05$, $p<0.05$ compared with mock transfectants) (Fig. 4A). TUNEL assay did not detect any significant difference in the number of apoptotic cells between CEACAM1 siRNA-transfectants and mock transfectants (Fig. 4A). In mock transfectants, actin filaments stained with phalloidin were mainly localized in the cell membrane and the area of cell-to-cell attachment (Fig. 4B). Significantly, in CEACAM1 siRNA-transfected cells, the cell membrane became wavy and protruded, and there was spotty distribution of actin filaments in the cytoplasm with accumulation at the leading edge of ruffled cell membranes (Fig. 4B).

siRNA-mediated inhibition of CEACAM1 in HepG2 cells in suspension culture

When HepG2 cells were cultured in suspension, the growth rate of CEACAM1-siRNA treated cells was significantly decreased compared with mock transfectants (siRNA#1 *vs.* siRNA#2 *vs.* mock; 1.5±0.4, 1.2±0.3, 3.0±0.5×10^5 cells/mL; $p<0.05$, $p<0.05$ compared with mock transfectants) (Fig. 5A). The mean BrdU labeling index in CEACAM1 siRNA-transfected HepG2 cells was relatively low compared with mock transfectants (siRNA#1 *vs.* siRNA#2 *vs.* mock; 36±7%, 27±11%, 51±4%; $p<0.05$, $p<0.05$ compared with mock transfectants). TUNEL assay detected no significant difference in the ratio of apoptotic cells between CEACAM1 siRNA-transfectants and mock transfectants (Fig. 5A). In both mock transfectants and CEACAM1-siRNA-treated cells, actin filaments were mainly localized in the area of cell-to-cell attachment (Fig. 5B). Mock transfectants took on a polygonal shape with smaller intercellular spaces, while CEACAM1-

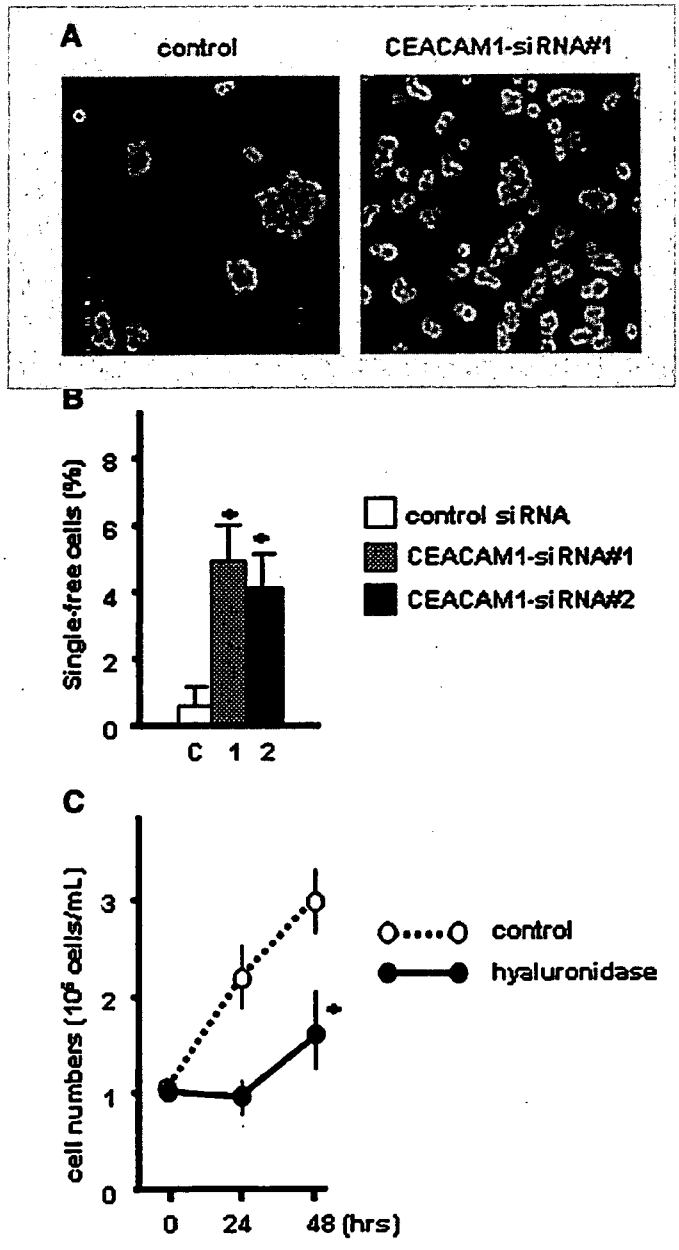

Fig. 6. Cell-aggregation assay. (A) Representative photograph of HepG2 cells after 2 h in suspension culture (magnifications: ×10). (B) Percentages of single cell populations. *C*, control siRNA-treated cells; 1, CEACAM1-siRNA#1-treated cells; 2, CEACAM1-siRNA#2-treated cells. Bars, S.D. (C) Growth curve of HepG2 cells (1×^{5} cells/mL) in suspension culture in the absence (control) or presence (hyaluronidase) of hyaluronidase. Points, mean; bars, S.D.; *$p<0.05$ vs. control.